

Optical investigation of strong electronic correlations: magnetism in semiconductor moire materials

Atac Imamoglu

ETH Zurich

Co-workers:

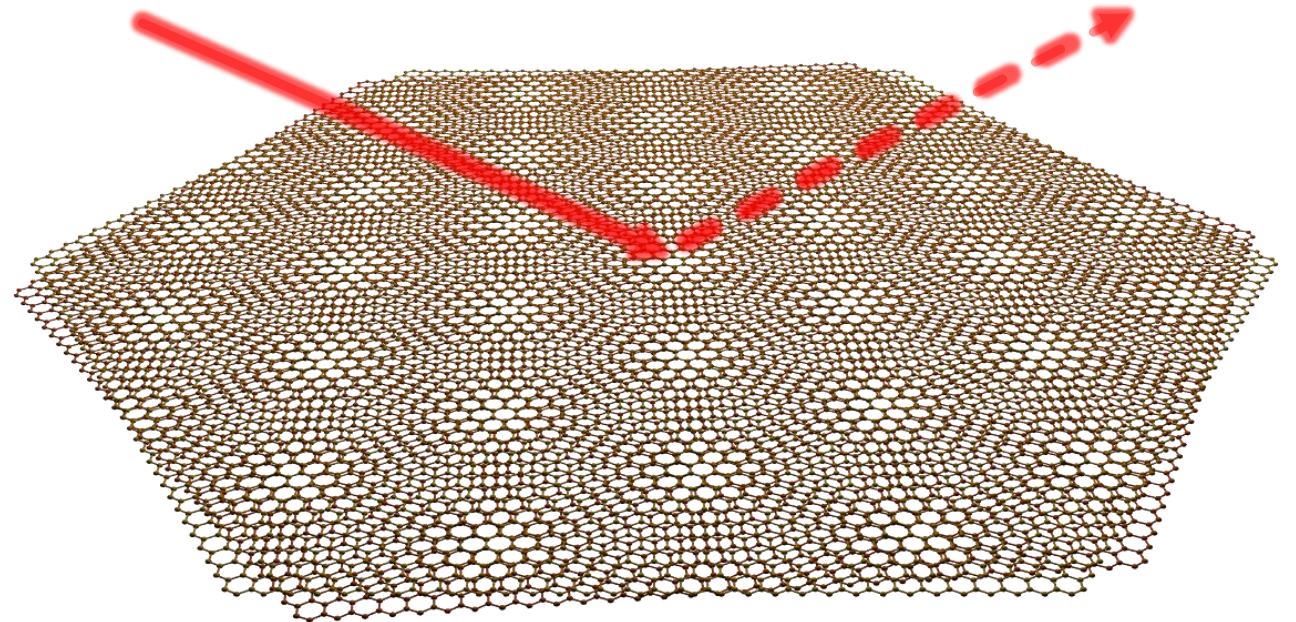
Livio Ciorciaro, Natasha Kiper,
Sarah Hiestand

Tomasz Smolenski, Martin Kroner

Ivan Morera, Eugene Demler

Yang Zhang (DFT calculations)

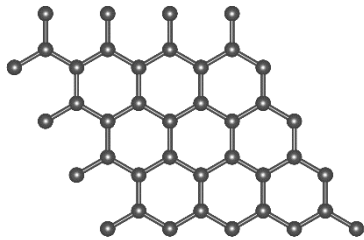
Kenji Watanabe, Takashi Taniguchi (NIMS)



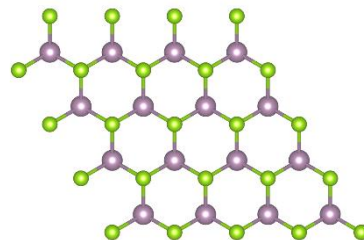
Emerging platform for studying strong correlations: van der Waals heterostructures

- Atomically-thin materials with different electronic, optical and magnetic properties can be combined to create a van der Waals heterostructure with novel hybrid functionality

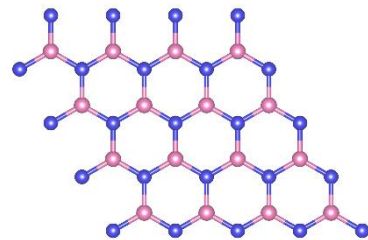
Graphene (metal)



TMD (semiconductor)

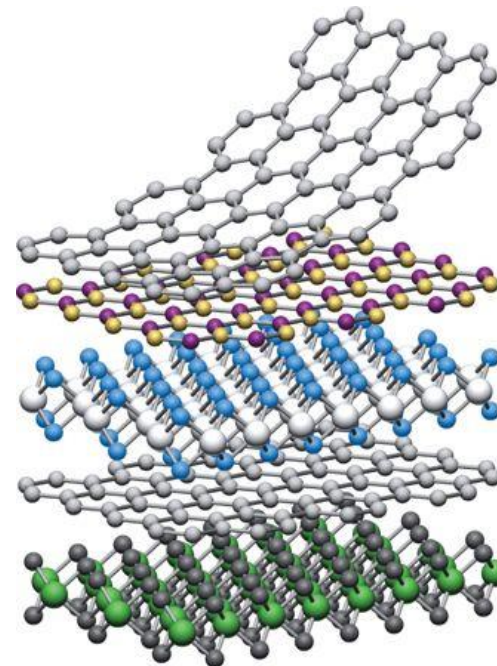


hBN (insulator)



Magnet, Superconductor, TI, ...

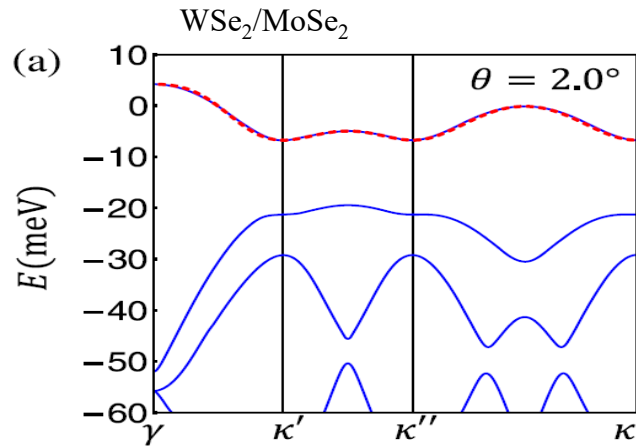
Van der Waals heterostructure



A. K. Geim *et al.*, Nature **499**, 419 (2013)

Moire fatbands in (twisted) semiconductor bilayers

Twisted bilayer transition metal dichalcogenide (TMD)



F. Wu *et al.*, Phys. Rev. Lett. **121**, 026402 (2018)

Heavy effective mass ($m^* \sim 0.7m_e$)

→ **Flat bands in wide range of angles**

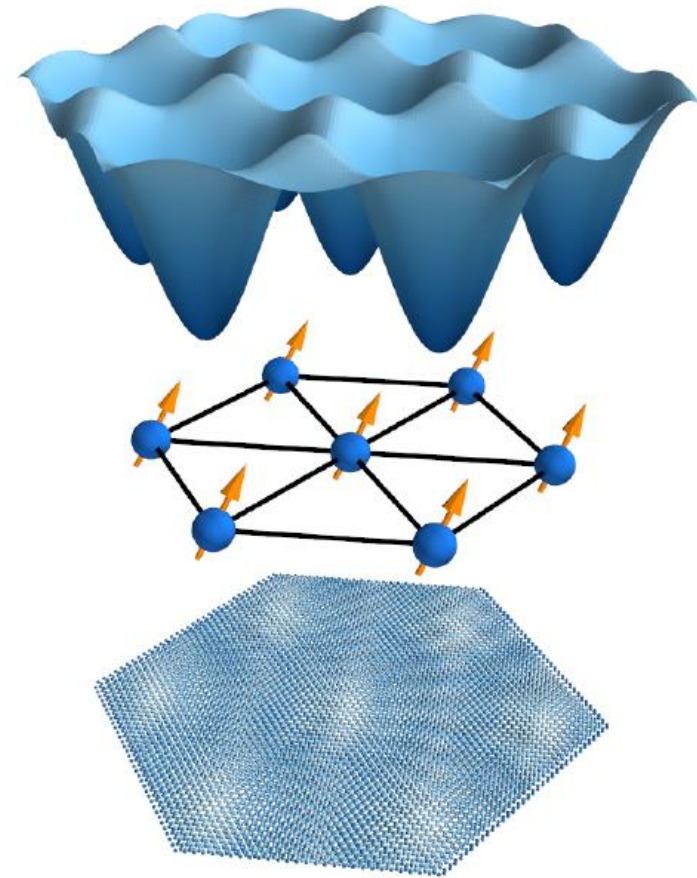
→ **Electric field tunable moire potential**

Difficulties

Electrical contact

Inhomogeneity due to strain

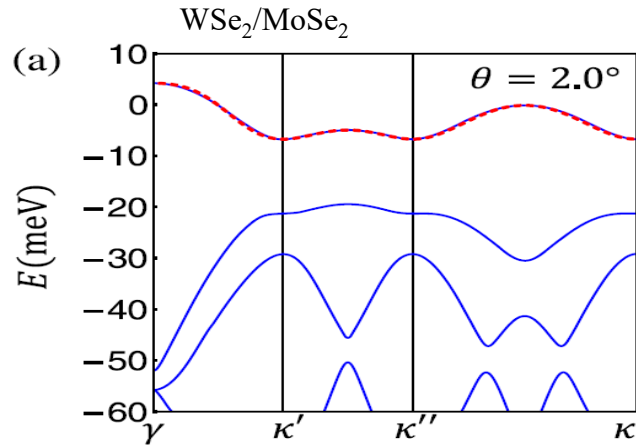
Local probe by optical spectroscopy



Mott-Wigner states & quantum anomalous Hall effect
(pioneering work: Wang and Mak-Shan groups)

Moire fatbands in (twisted) semiconductor bilayers

Twisted bilayer transition metal dichalcogenide (TMD)



F. Wu *et al.*, Phys. Rev. Lett. **121**, 026402 (2018)

Heavy effective mass ($m^* \sim 0.7m_e$)

→ **Flat bands in wide range of angles**

→ **Electric field tunable moire potential**

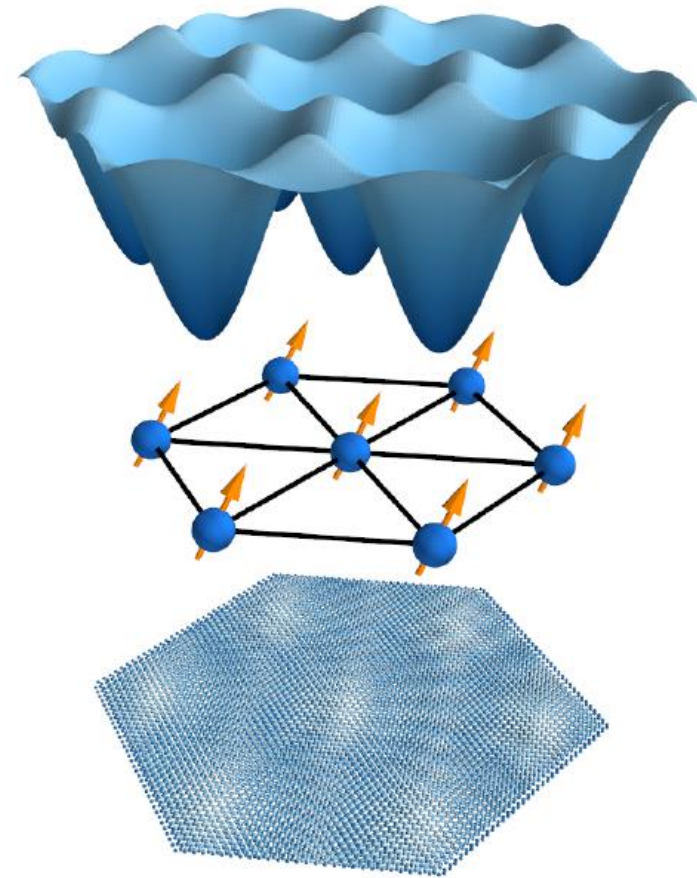
Difficulties

Electrical contact

Inhomogeneity due to strain

Local probe by optical spectroscopy

Mott-Wigner states & quantum anomalous Hall effect
(pioneering work: Wang and Mak-Shan groups)

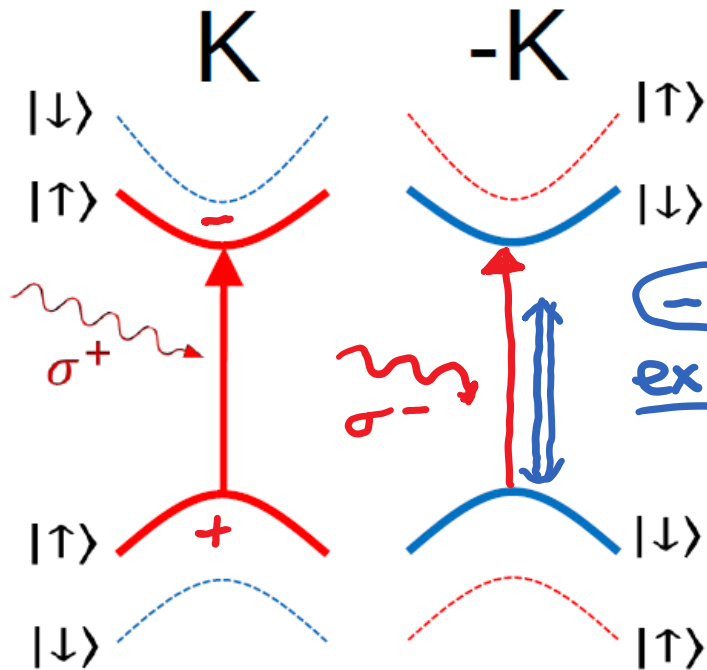


Quantum magnetism of correlated electrons:
120 Neel order or spin liquid or ...?

Outline

- Optics/excitons as a spectroscopic tool for investigating ground-state electronic properties
- Kinetic magnetism in semiconductor moire materials: magnetism that stems from kinetic energy minimization, instead of interactions

Materials: Transition metal dichalcogenides (TMD) -layered 2D valley semiconductors



exciton: bound state of an electron & a hole

Strong exciton resonance below the band-gap dominates the absorption/reflection & emission spectrum

Valley and spin are locked:
low energy K valley states
have spin-up

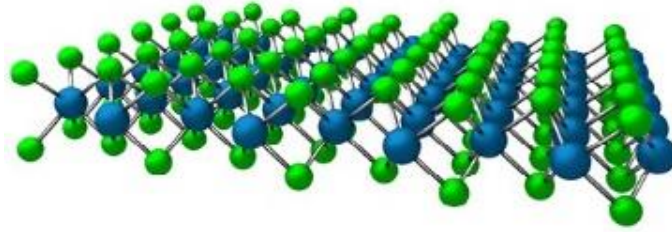
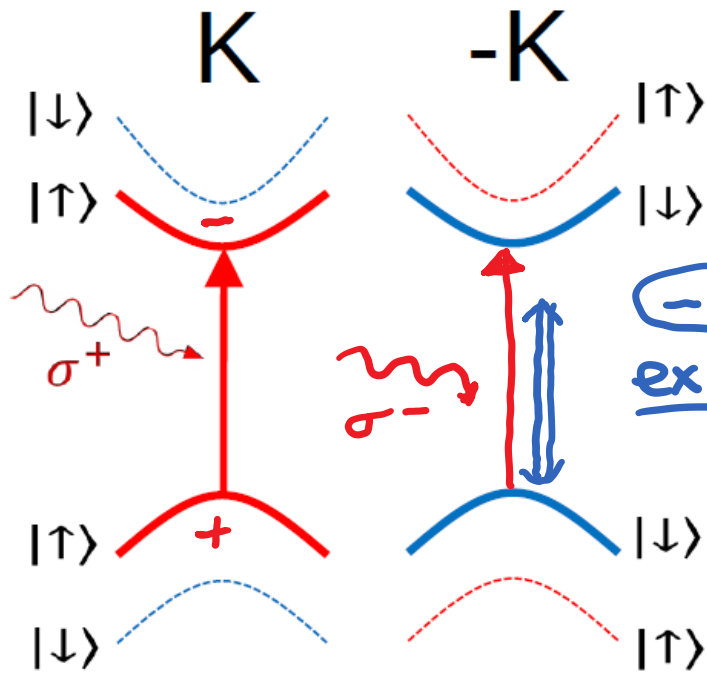
Table 1 Fundamental optoelectronic material parameters of monolayer TMD semiconductors

Material	m_r (m_0)	E_b (meV)	E_{gap} (eV)	κ	r_0 (nm)	r_{1s} (nm)
hBN MoS ₂ hBN	0.275 ± 0.015	221	2.160	4.45	3.4	1.2
hBN MoSe ₂ hBN	0.350 ± 0.015	231	1.874	4.4	3.9	1.1
hBN MoTe ₂ hBN	0.360 ± 0.040	177	1.352	4.4 ^a	6.4	1.3
hBN WS ₂ hBN	0.175 ± 0.007	180	2.238	4.35	3.4	1.8
hBN WSe ₂ hBN ^b	0.20 ± 0.01	167	1.890	4.5	4.5	1.7

Experimentally determined values of the exciton reduced mass m_r , the 1s exciton binding energy E_b , the free-particle bandgap E_{gap} , the dielectric screening parameters r_0 and κ , and the root-mean-square radius of the 1s exciton r_{1s} . Typical error bars on experimental values of E_b and E_{gap} are ±3 meV. Typical error bars on values of r_0 and r_{1s} are ±0.1 nm, except for MoTe₂, where they are ±0.3 nm.
^aThe value of κ for MoTe₂ is assumed to be 4.4 and is not a fitting parameter (see text for details).
^bValues for hBN-encapsulated WSe₂ are taken from ref. ²⁷

Materials: Transition metal dichalcogenides (TMD)

-monolayer valley semiconductors



exciton: bound state of an electron & a hole


Strong exciton resonance below the band-gap dominates the absorption/reflection & emission spectrum

Implications of small Bohr radius
($a_B \sim 1 \text{ nm}$)


- robust quantum impurity (exciton is wavefunction unaffected by exciton-electron interactions)
- fast radiative decay of excitons: $\Gamma_x \propto 1/a_B^2$

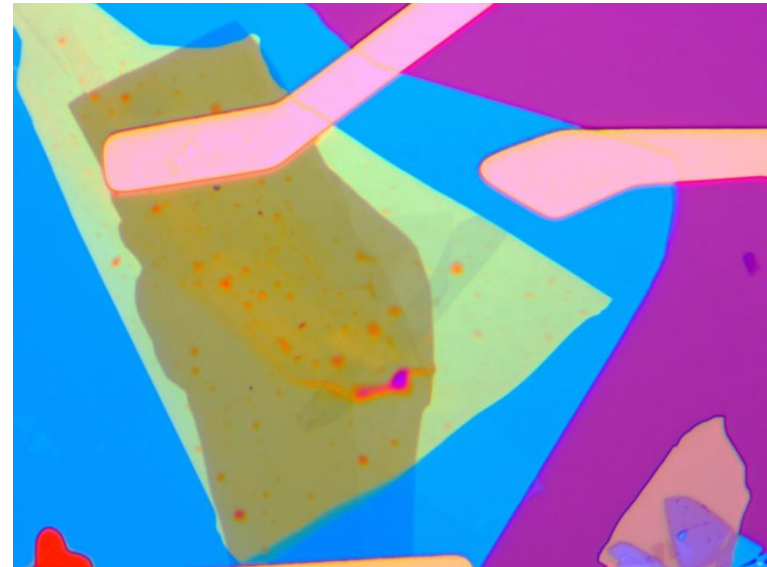
Monolayer MoSe₂ device with tunable charge density



 Graphene (few layers)

 MoSe₂

 hBN (30-35nm)

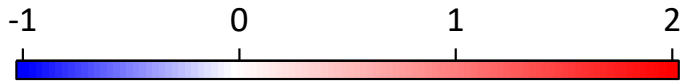


Elementary optical excitations in monolayer MoSe₂

Charge neutrality:

tightly bound 1s exciton dominates

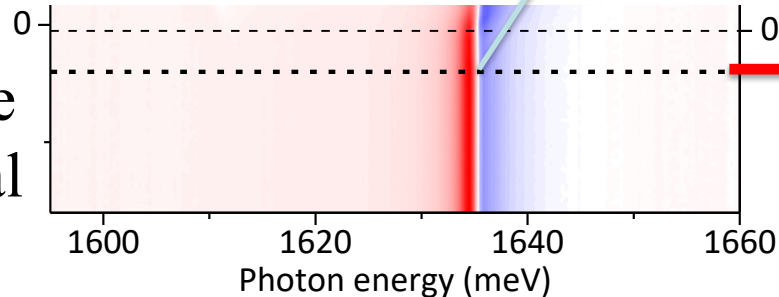
Reflectivity



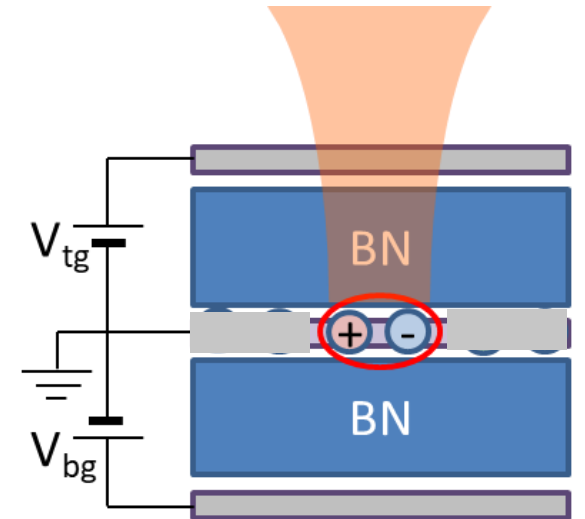
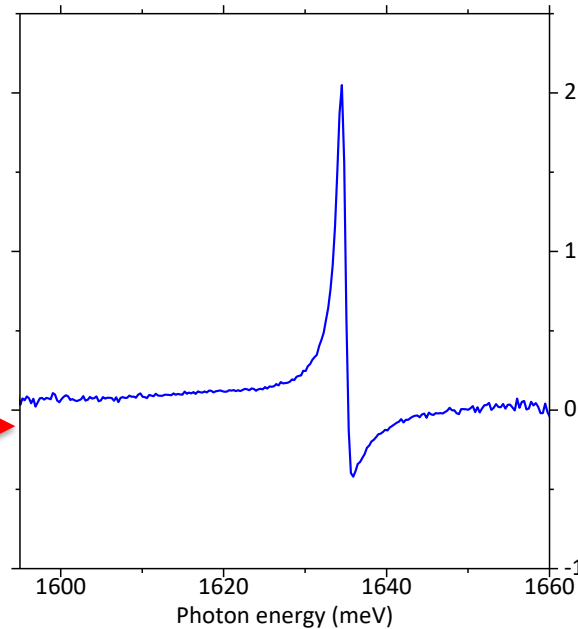
Exciton

Gate voltage V_t (V)

charge neutral



Electron density n_e (10^{12} cm^{-2})



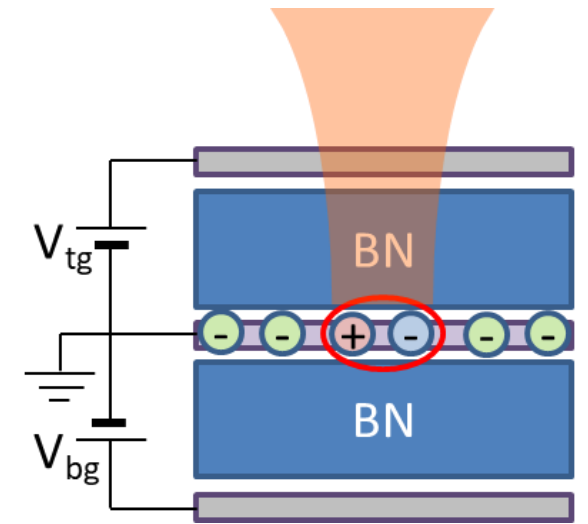
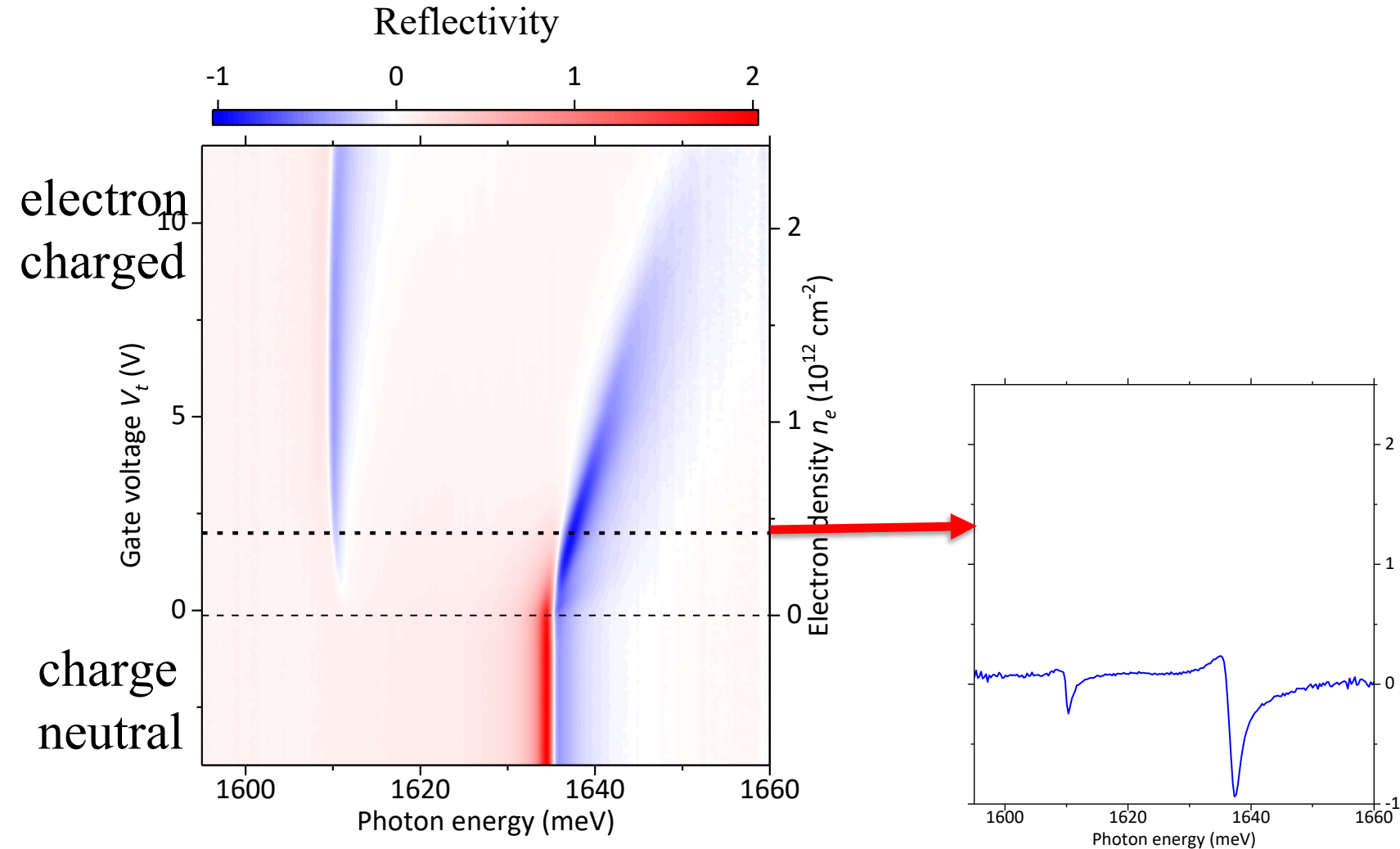
Elementary optical excitations in monolayer MoSe₂

Charge neutrality:

tightly bound 1s exciton dominates

Finite electron or hole density:

spectrum is drastically modified

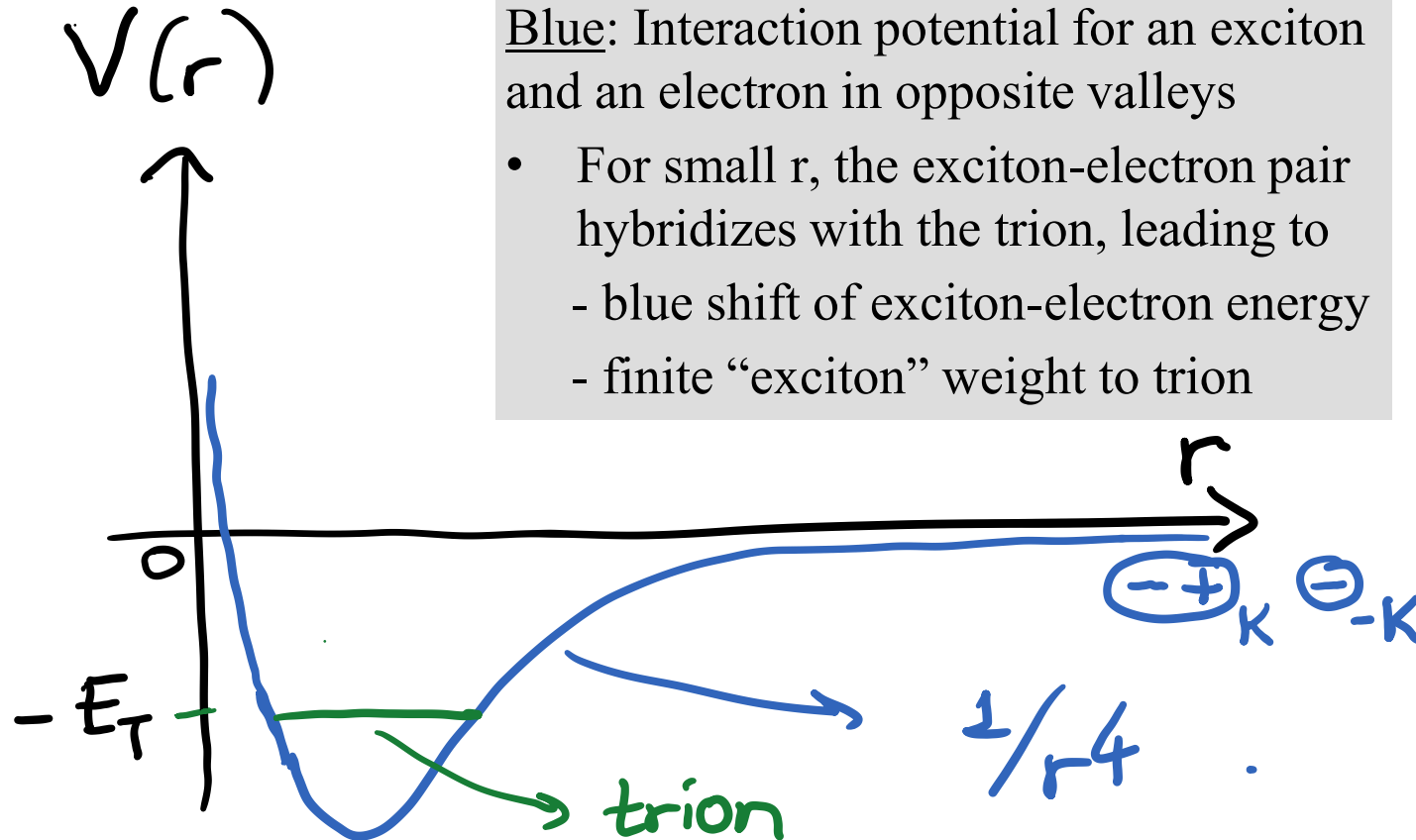


How to understand the modified spectrum: Exciton-electron scattering in a monolayer TMD

- Excitons interact with itinerant electrons or holes from the opposite valley and form a bound molecular state termed "trion"

Blue: Interaction potential for an exciton and an electron in opposite valleys

- For small r , the exciton-electron pair hybridizes with the trion, leading to
 - blue shift of exciton-electron energy
 - finite "exciton" weight to trion



exciton $\ominus \oplus$
 electron \ominus
 $r =$ separation of
 an exciton & electron

A free electron-exciton pair:
 blue-shift - effective repulsive interaction
Excitons injected below the trion resonance:
 red-shift - effective attractive interaction

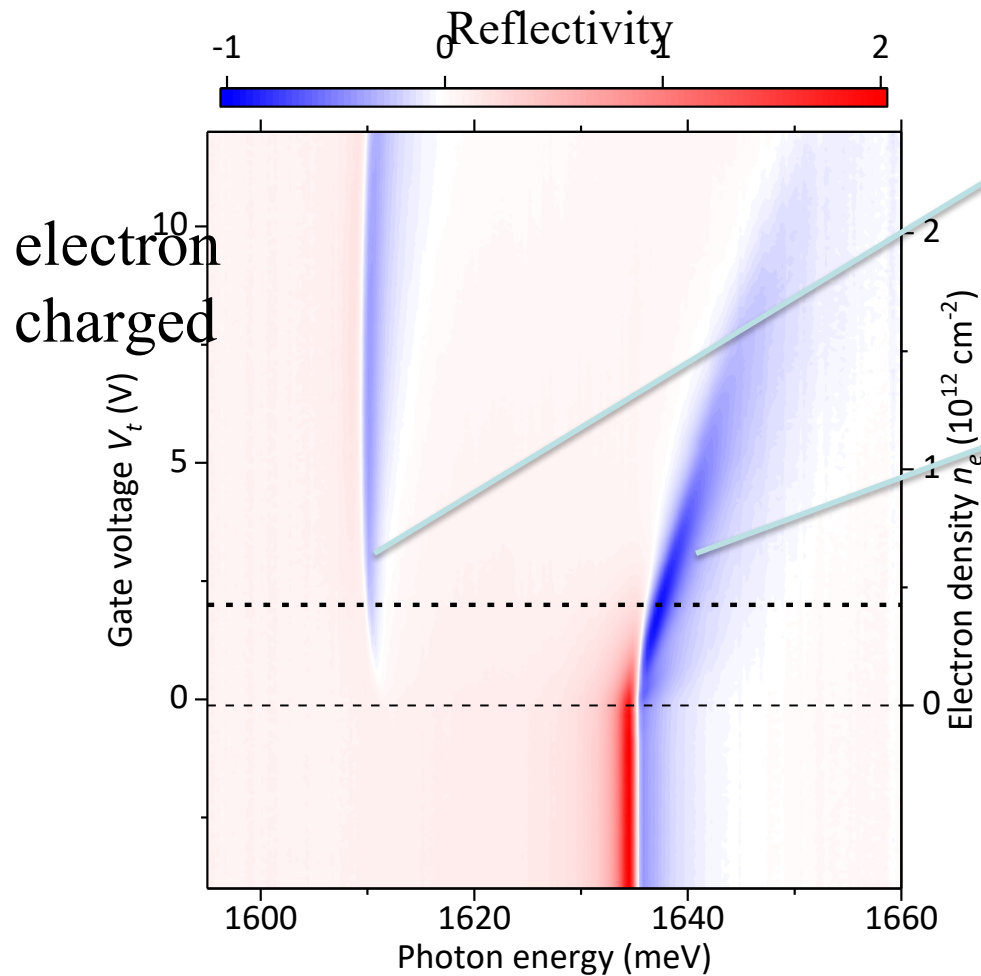
Elementary optical excitations in monolayer MoSe₂

Charge neutrality:

tightly bound 1s exciton dominates

Finite electron or hole density:

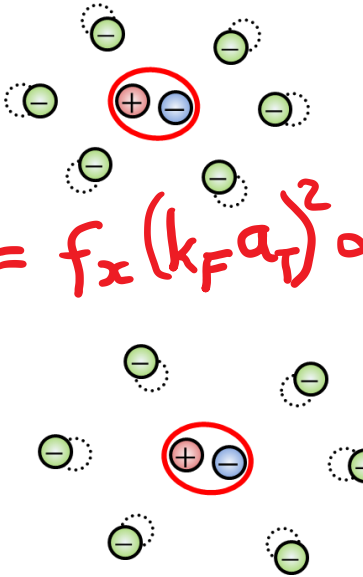
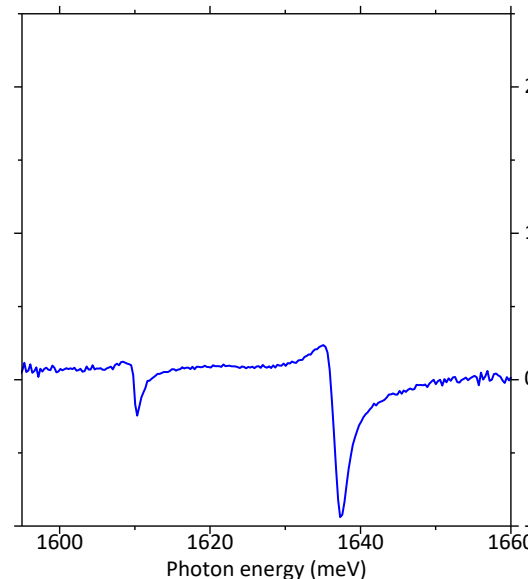
exciton-polarons (many-body excitations)



Attractive-polaron (AP)

AP oscillator strength: $f_{AP}^K = f_x (k_F a_T)^2 \propto n_{elec}^{K'}$

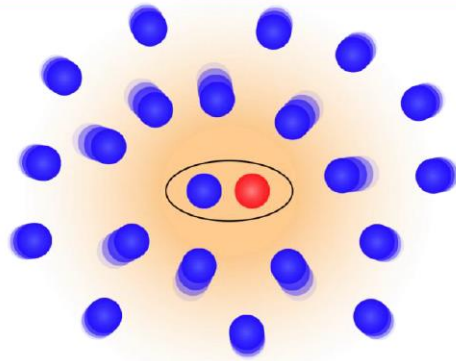
Repulsive-polaron (RP)



Energy shift of Exciton
(Repulsive polaron)
→ Charge sensing

Attractive polaron as an electronic spin sensor in MoSe₂ monolayer

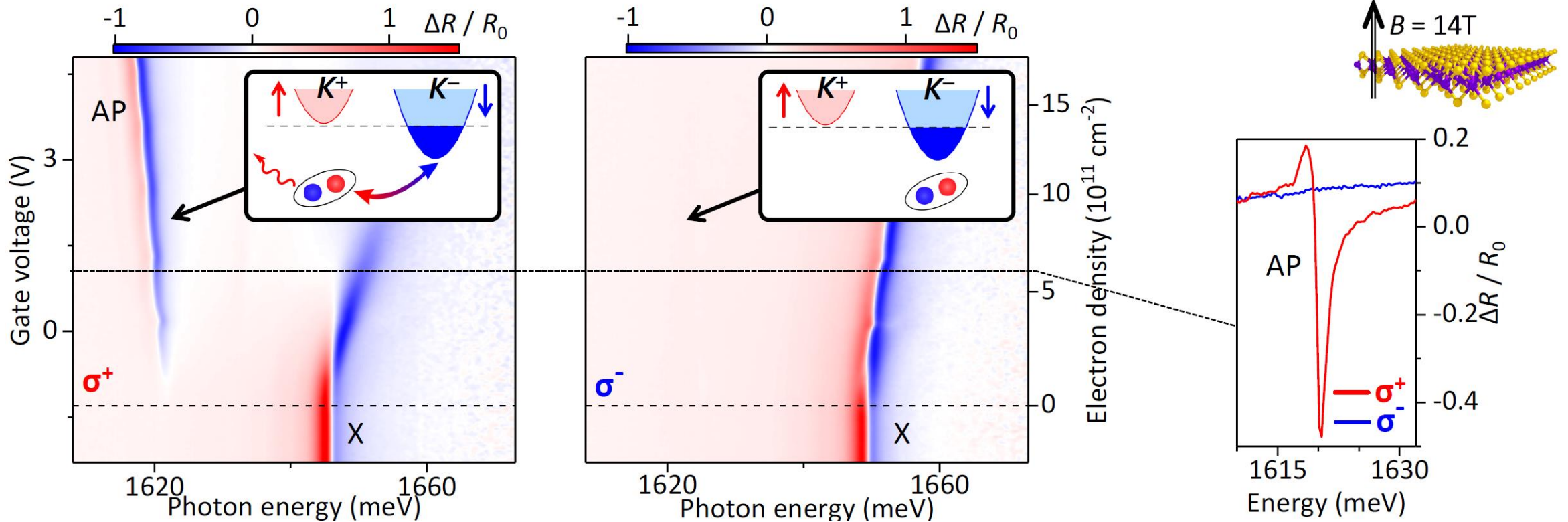
Attractive polaron (AP)



- Collective trion excitation
- Oscillator strength f_{AP} proportional to the electron density

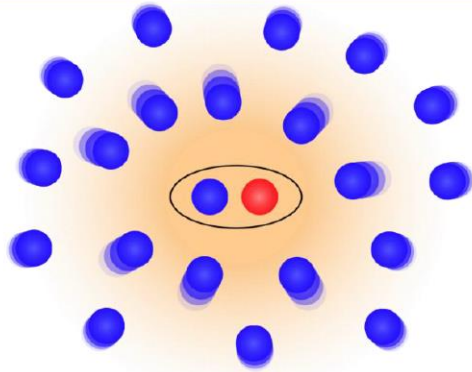
$$f_{AP}^{\pm} = f_X \cdot (4\pi a_T^2) \cdot n_e^{\mp}$$

Due to large spin-orbit coupling at K, K' valleys, spin and valley are locked



Attractive polaron as an electronic spin sensor in MoSe₂ monolayer

Attractive polaron (AP)

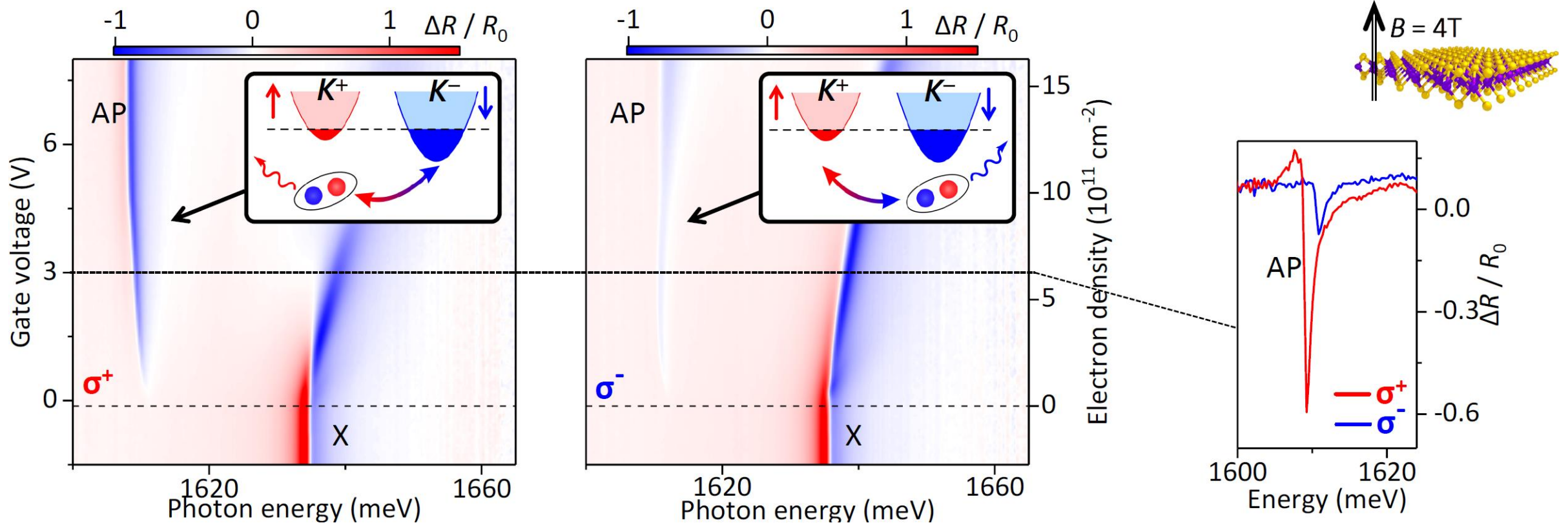


- Collective trion excitation
- Oscillator strength f_{AP} proportional to the electron density

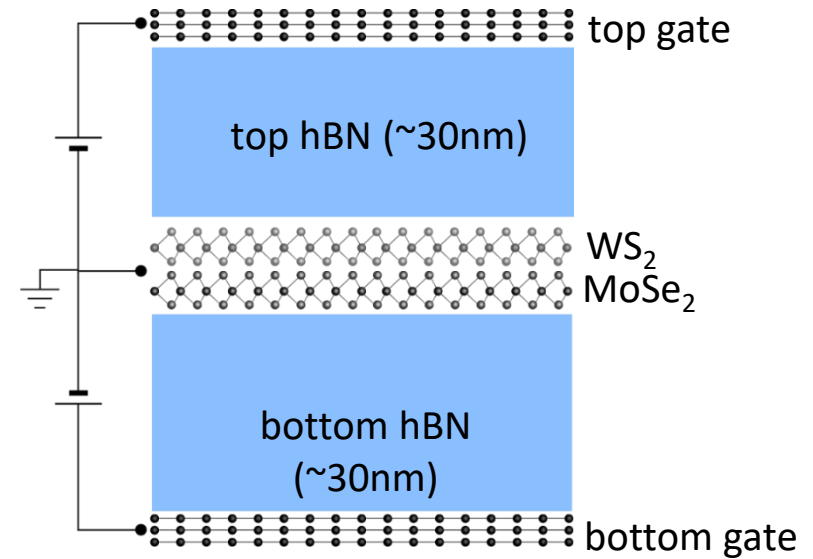
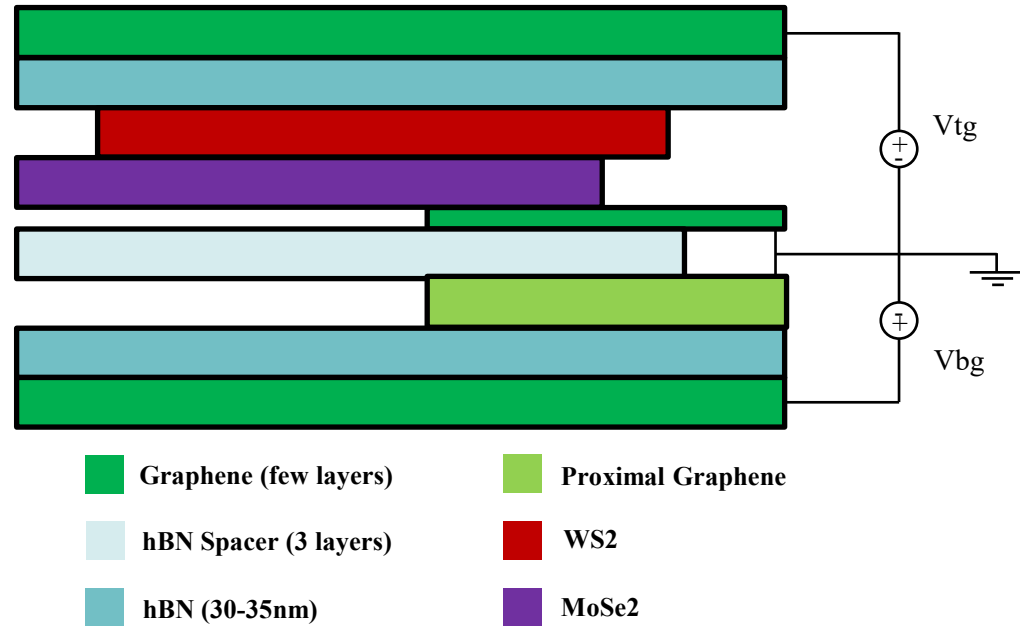
$$f_{AP}^{\pm} = f_X \cdot (4\pi a_T^2) \cdot n_e^{\mp}$$

- AP circular polarization degree directly corresponds to electron spin polarization degree

$$s = \frac{n_e^- - n_e^+}{n_e^- + n_e^+} = \frac{f_{AP}^+ - f_{AP}^-}{f_{AP}^+ + f_{AP}^-}$$

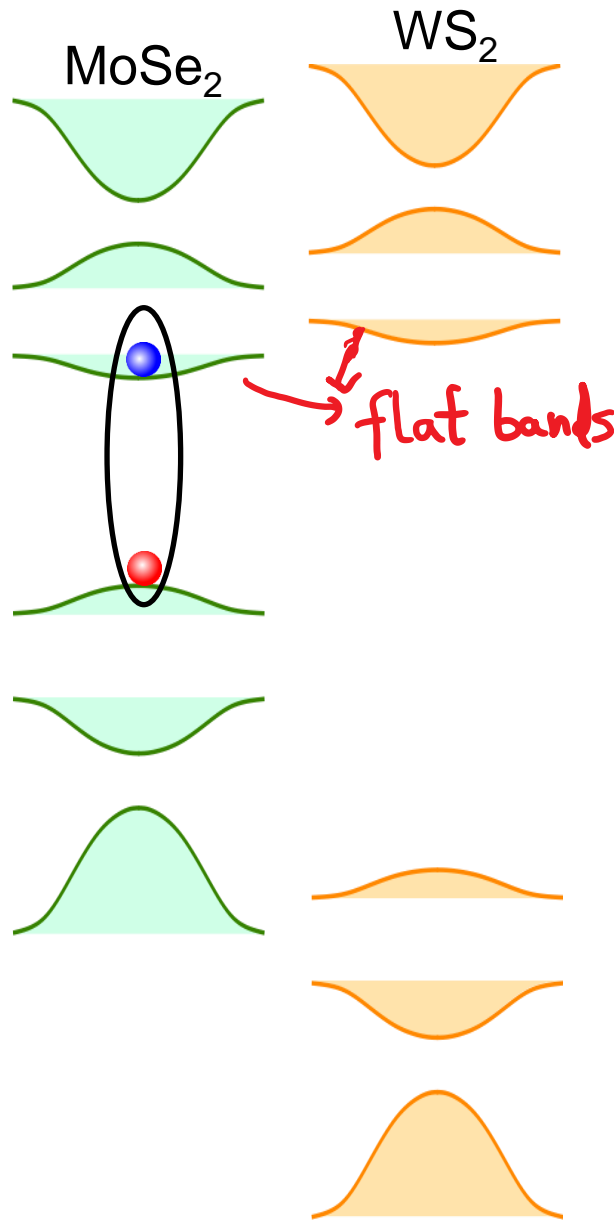


A semiconducting moire system: MoSe₂/WS₂

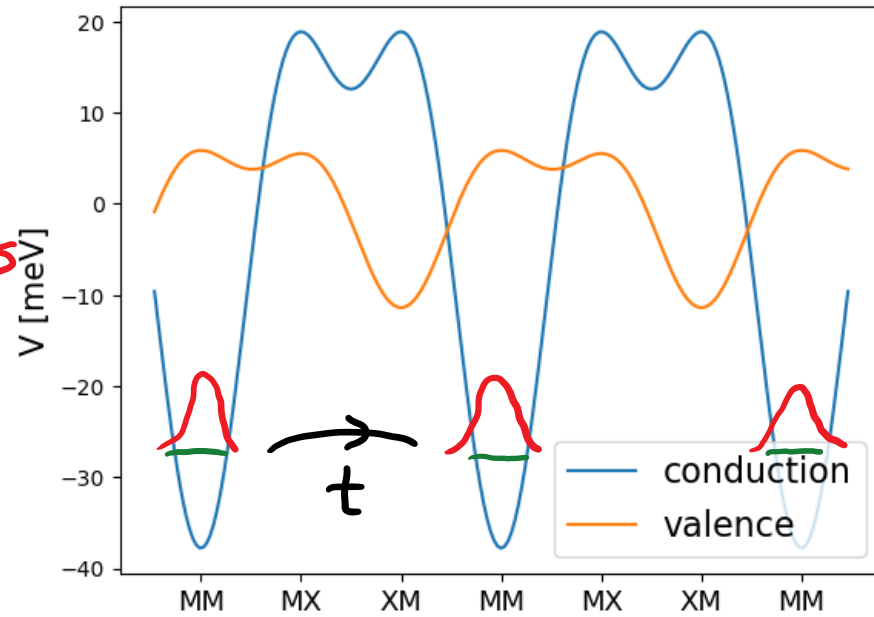


- Moire potential due to lattice mismatch of $\sim 4\%$
- Type I band alignment – both CB minimum and VB maximum are in MoSe₂
- Electronic bands are trivial but E-field tuning may yield Chern bands

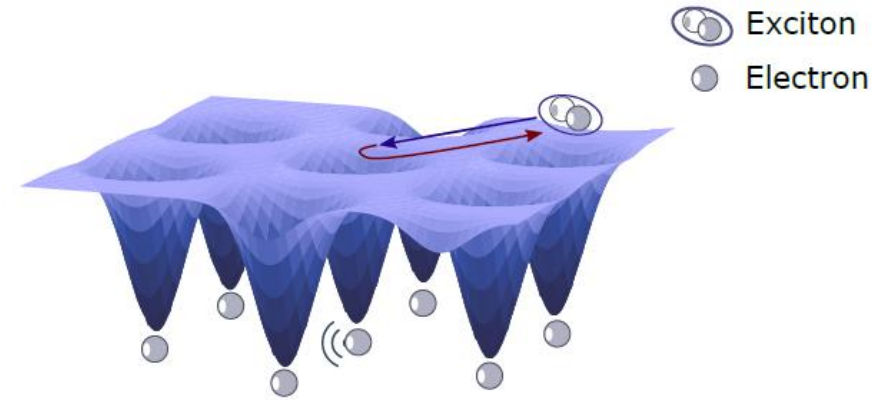
A semiconducting moire system: MoSe₂/WS₂



(Yang Zhang)

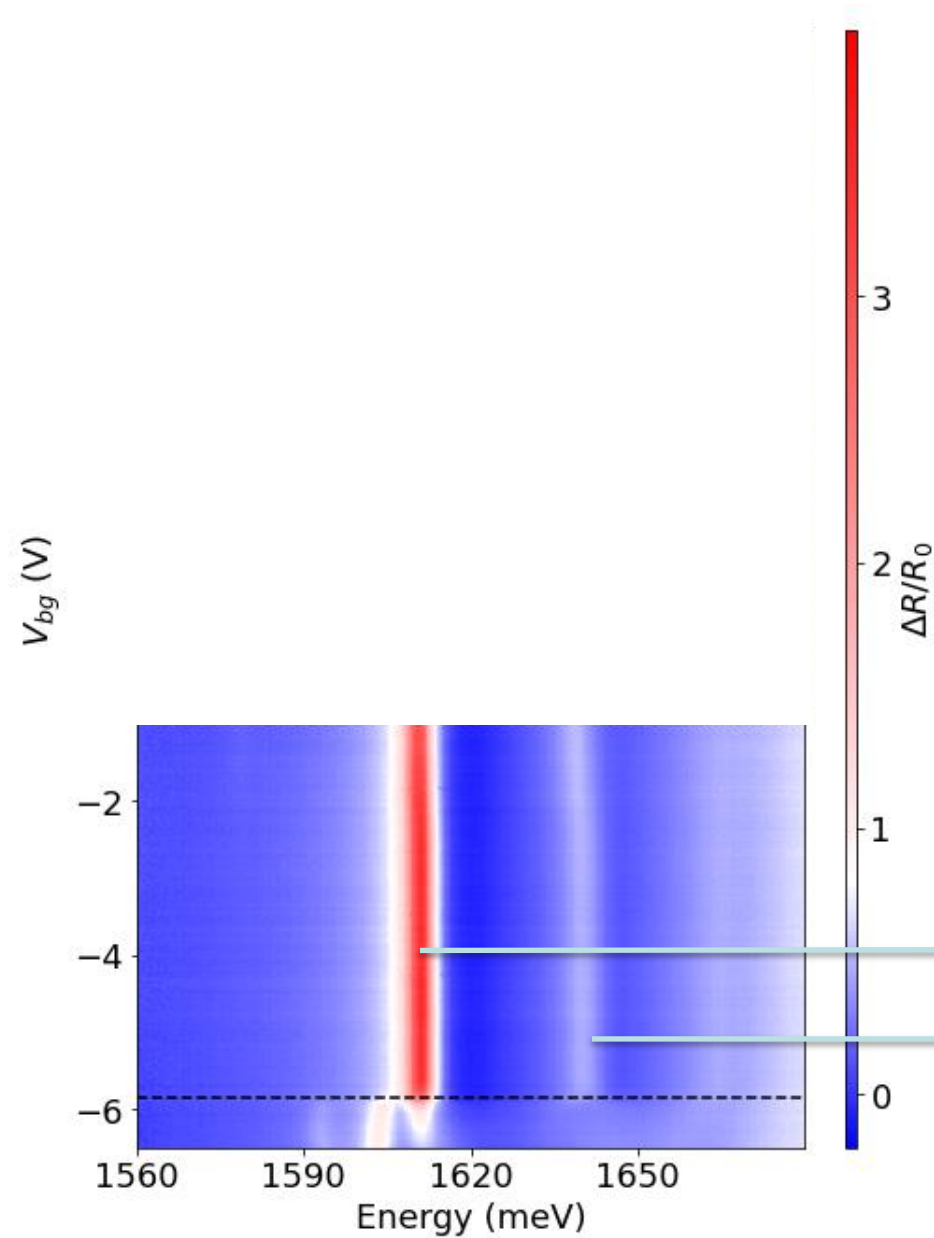
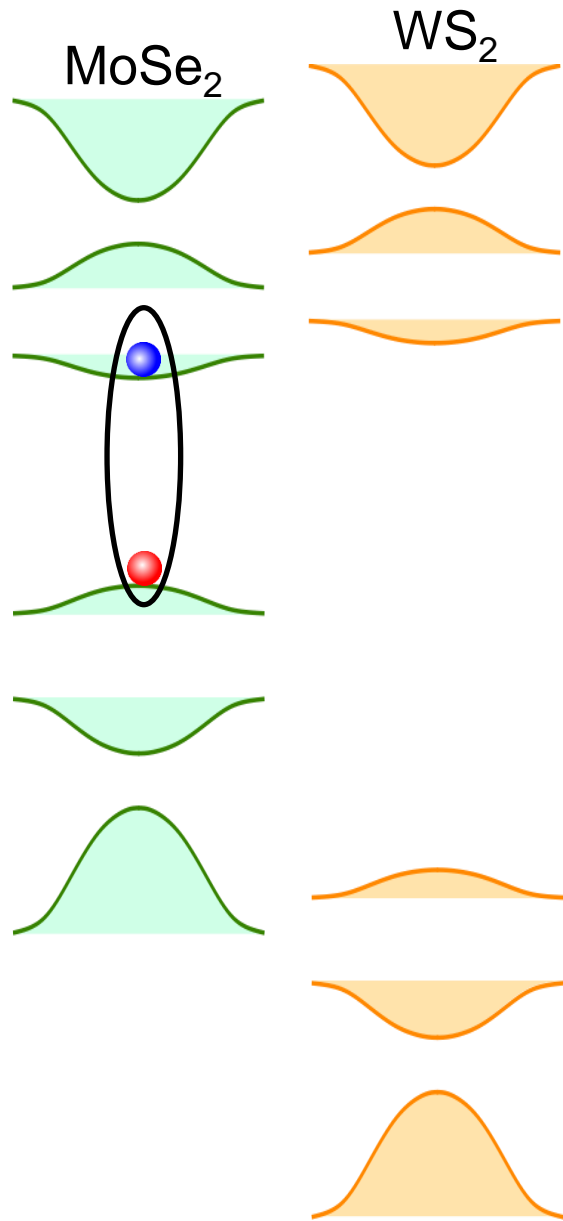


$U_{on-site}^c \sim 50 \text{ meV}$
 hopping: $t \sim 1 \text{ meV}$



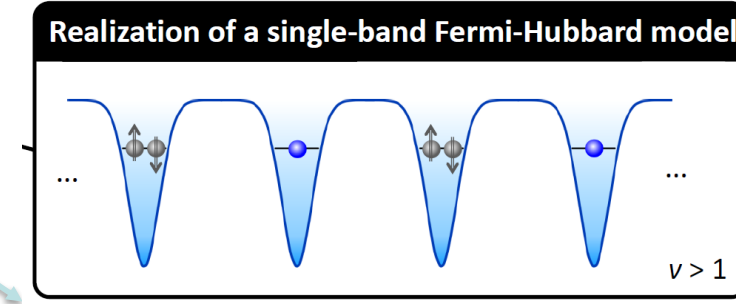
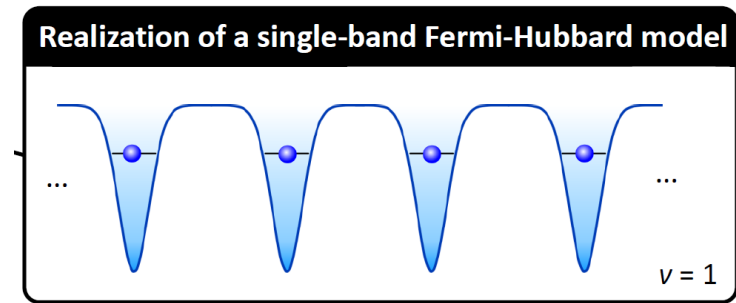
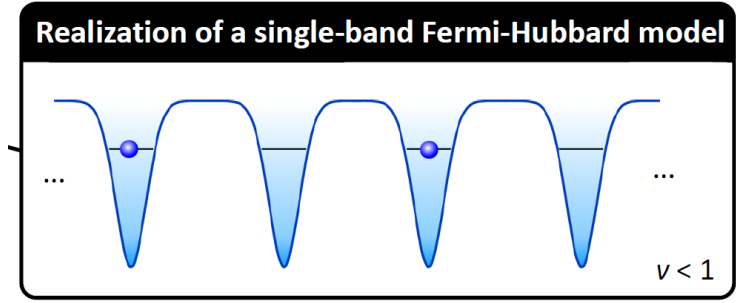
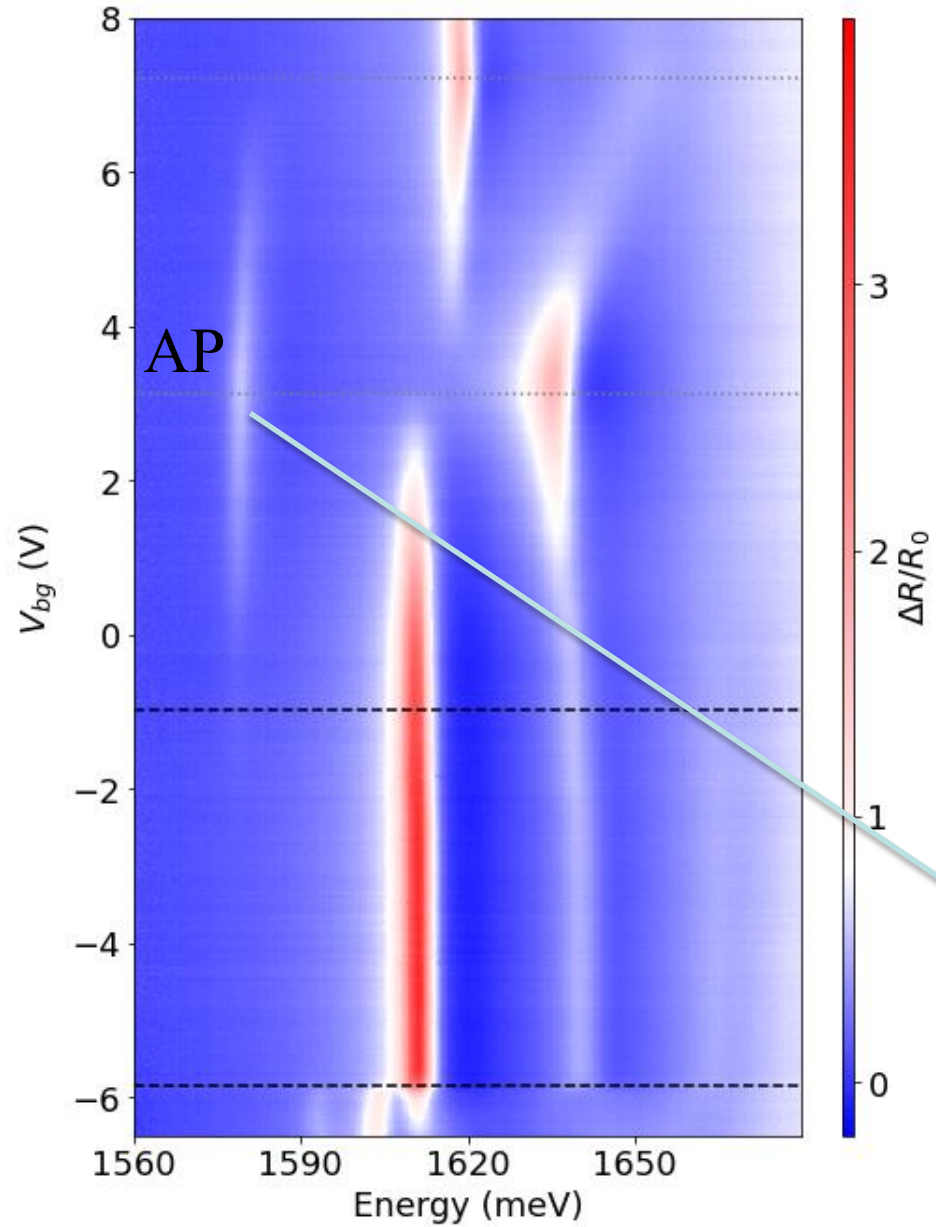
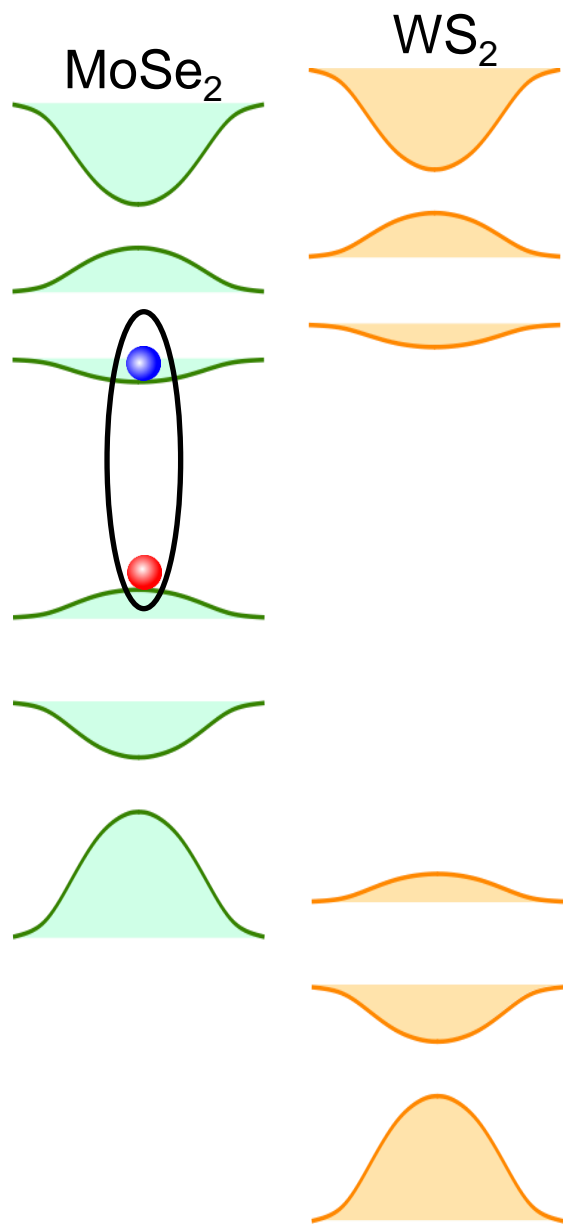
- Potential landscape for electrons and excitons are generically different.

Semiconductor moire system: MoSe₂/WS₂



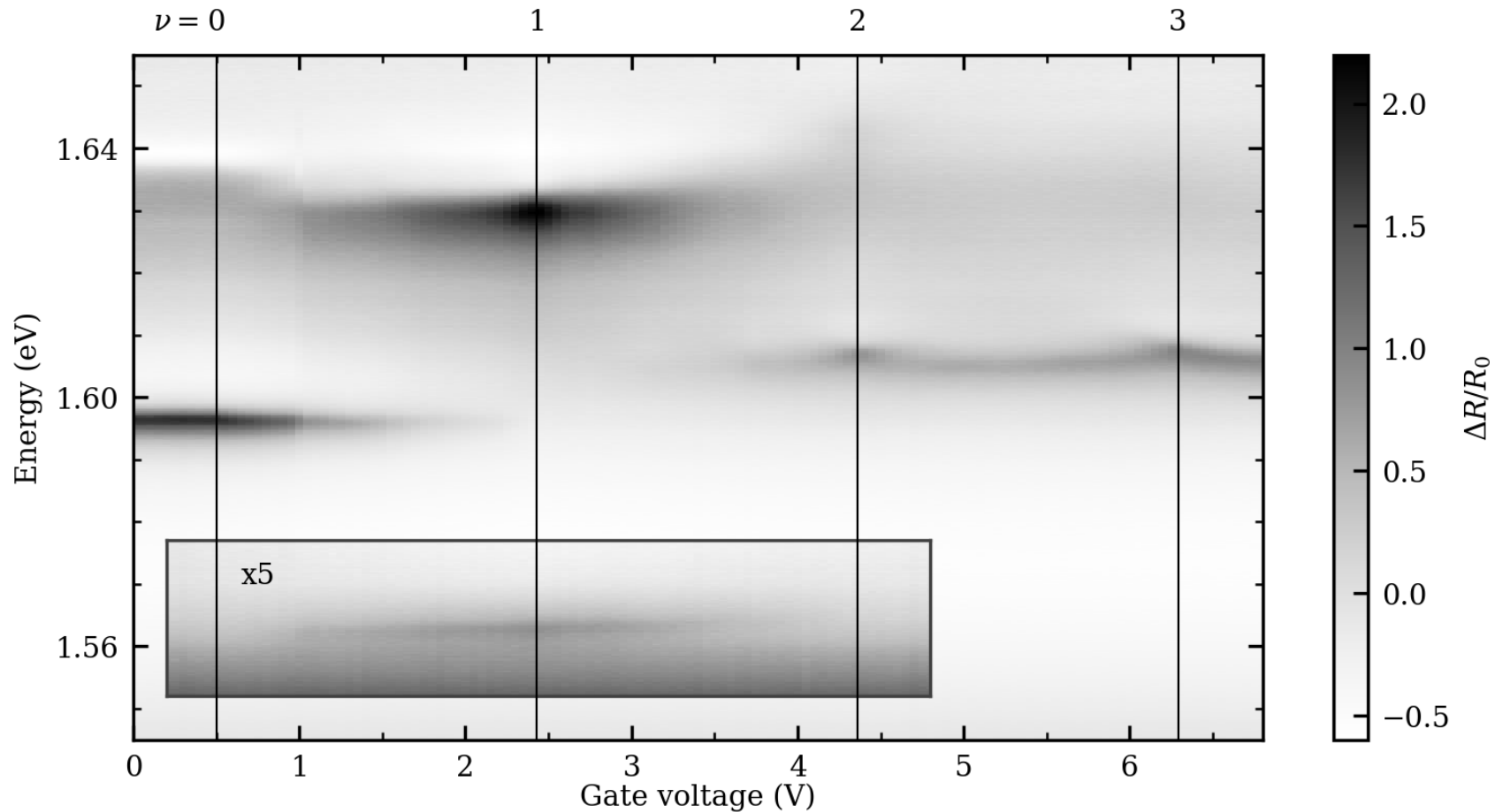
Moiré excitons: periodic potential leads to formation of flat exciton bands in charge neutrality

Semiconductor moire system: MoSe₂/WS₂



Attractive polaron: dressing of lowest energy moire exciton by electrons strongly localized on moire lattice sites

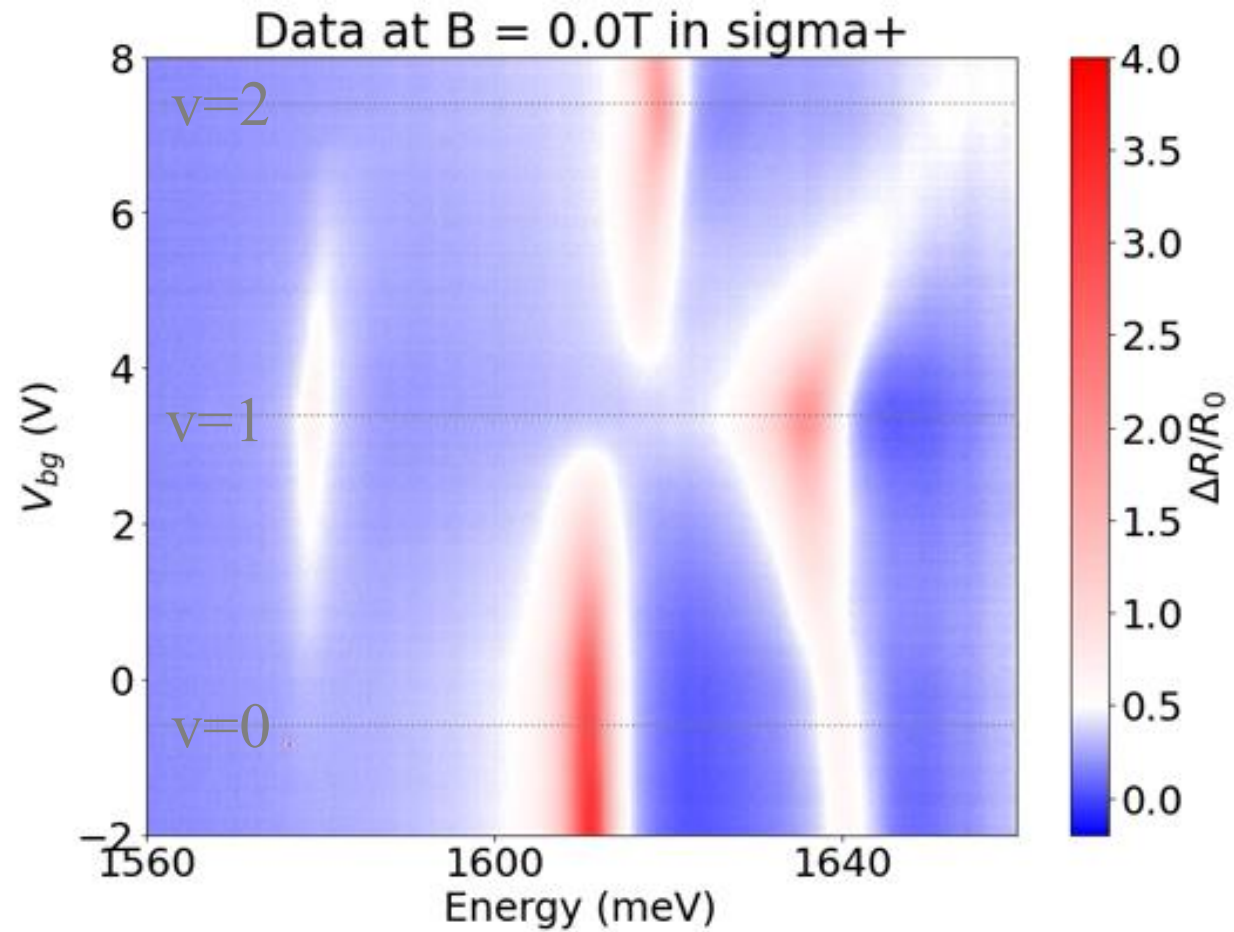
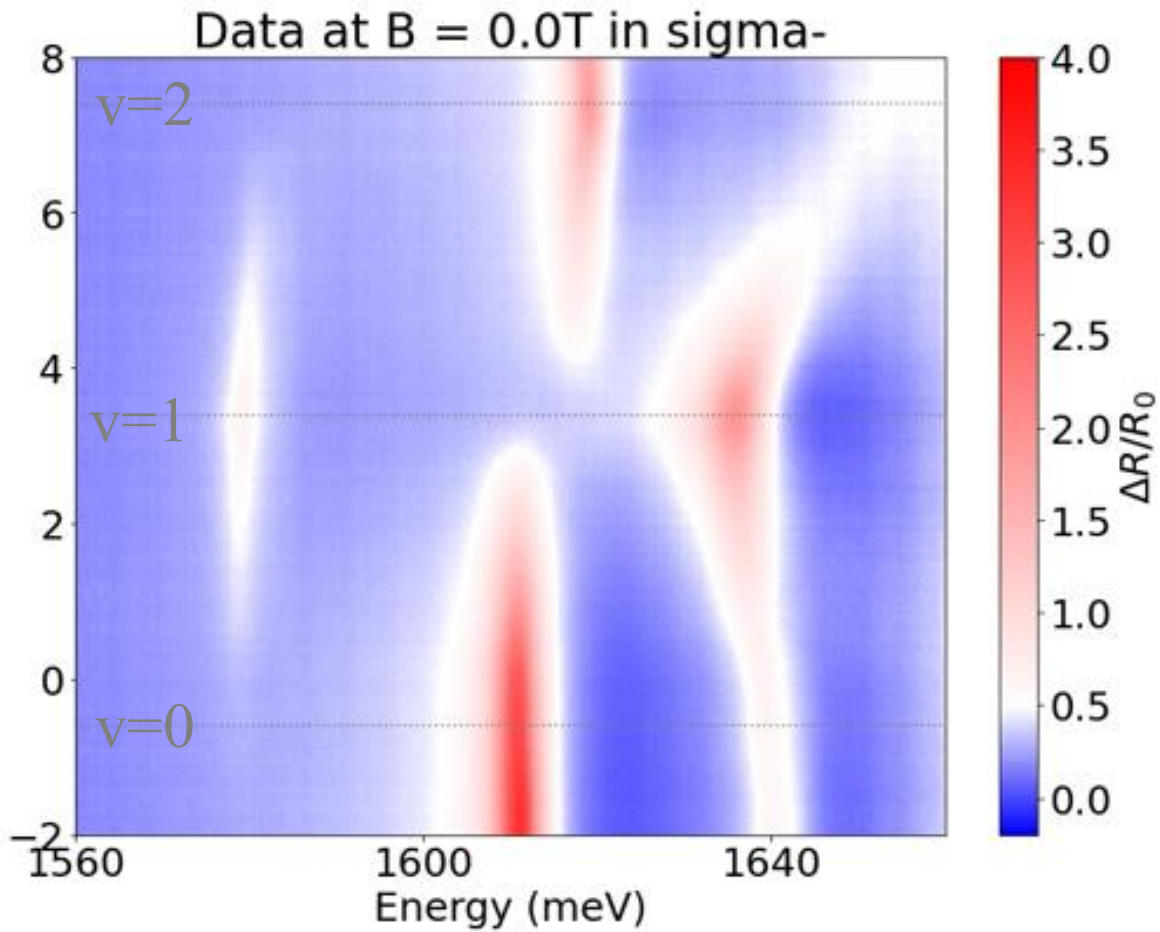
Semiconductor moire system: $\text{MoSe}_2/\text{WS}_2$: Second device



Cusps in reflection for $\nu = 2$ and $\nu = 3$ signaling incompressible electronic states even at high doping

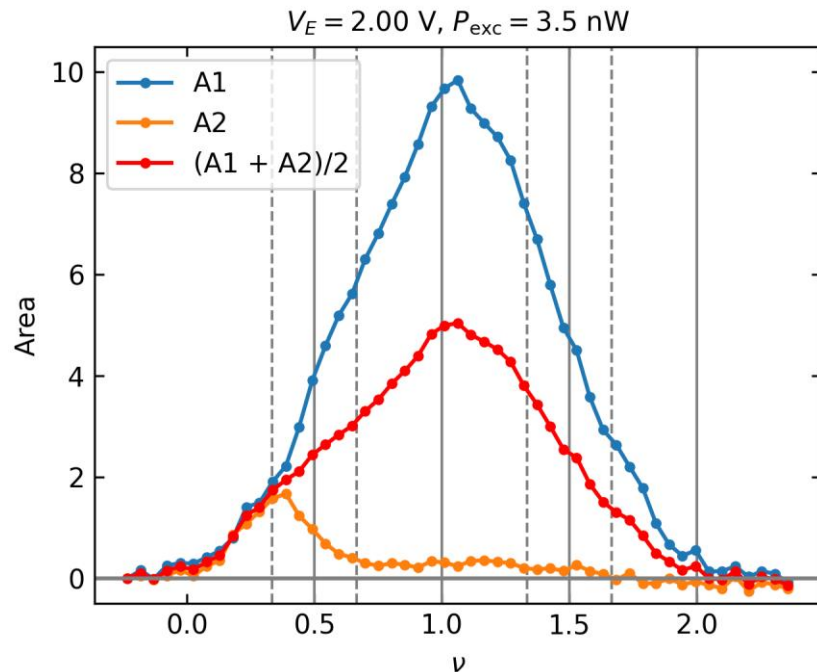
Magnetic field response at T=4 K

To explore magnetic properties, we determine magnetization as a function of temperature and magnetic field

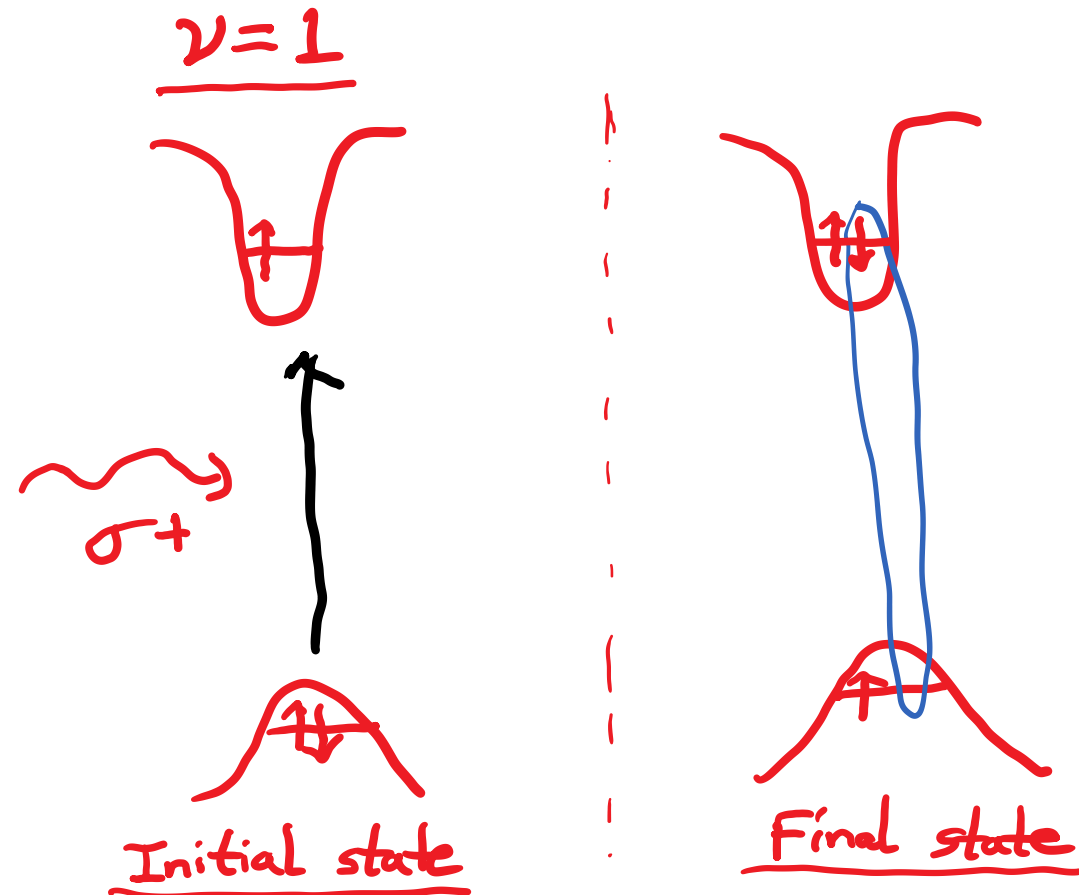


Evidence for the (extended) single-band Hubbard model

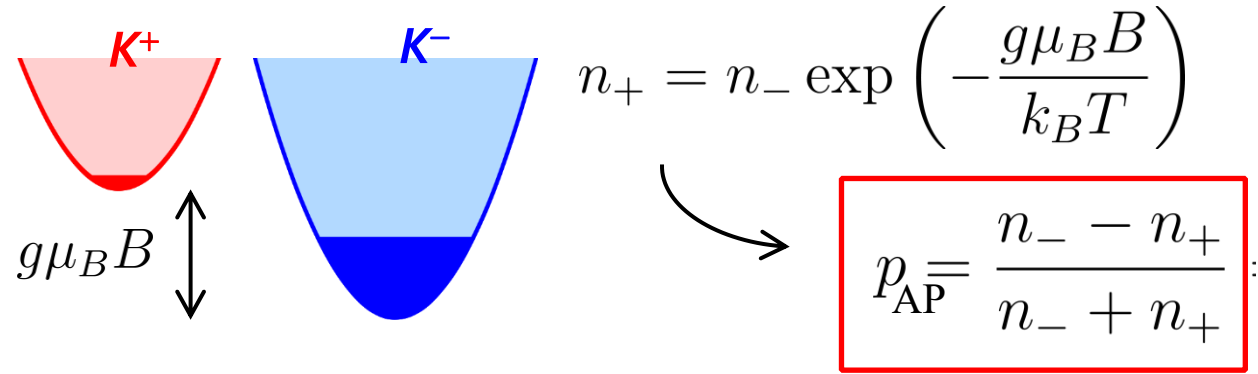
- For $B=4T$, electrons are spin-valley polarized in K' -valley; the strength of K -valley AP increases linearly till $\nu=1$ and then decreases linearly; for $\nu=2$, all electronic states in the lowest moire flat band are filled and they cannot contribute to AP/trion formation.



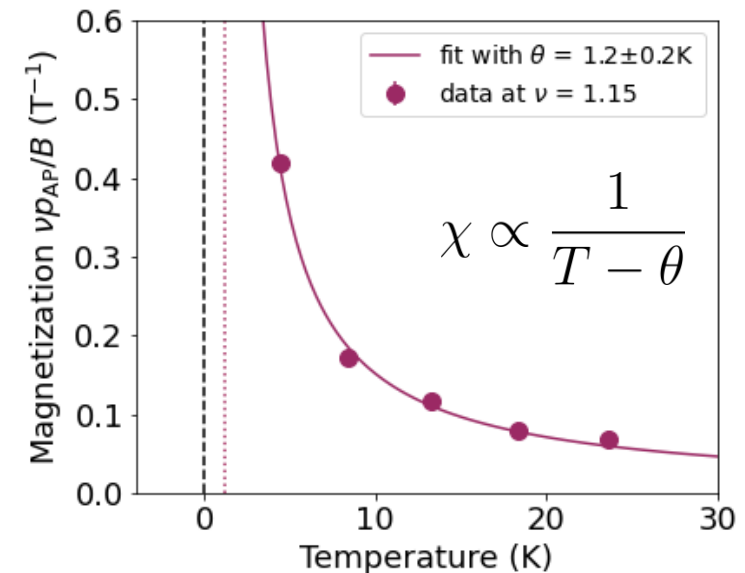
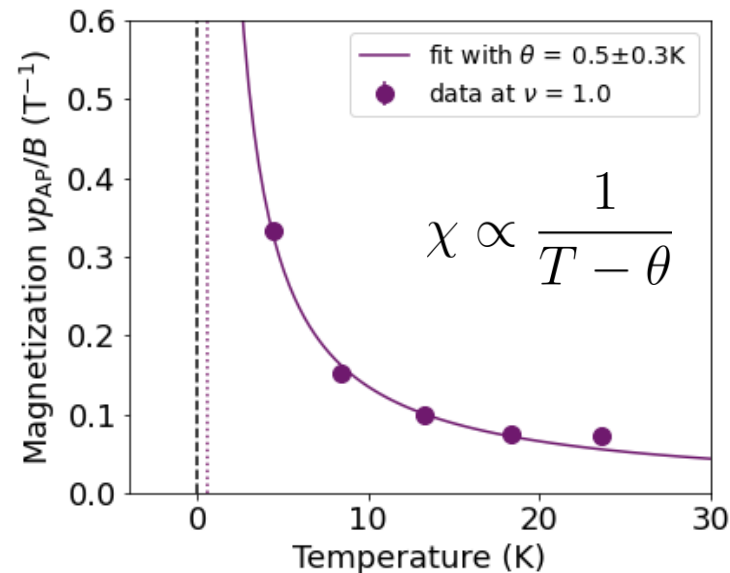
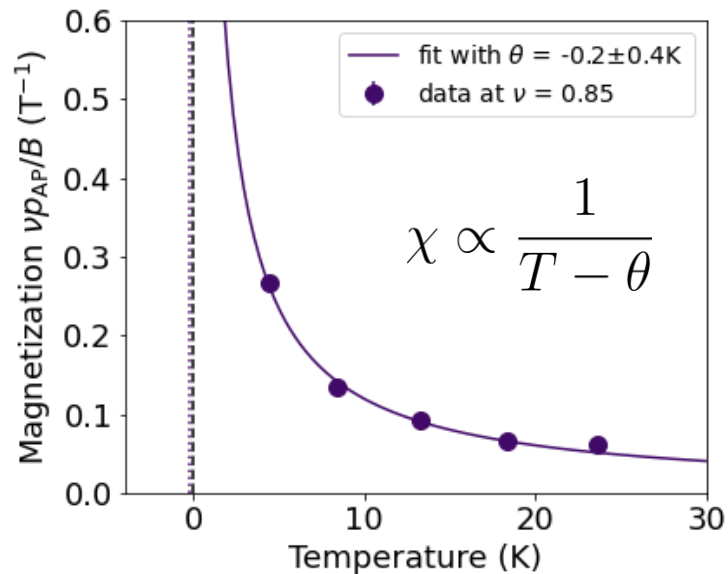
A1: strength of K -valley ($\sigma+$ polarized) AP
 A2: strength of K' -valley ($\sigma-$ polarized) AP



Direct measurement of magnetization (p_{AP}) using attractive polarons



Spin susceptibility: $\chi \propto \lim_{B \rightarrow 0} \nu \frac{p_{AP}}{B}$

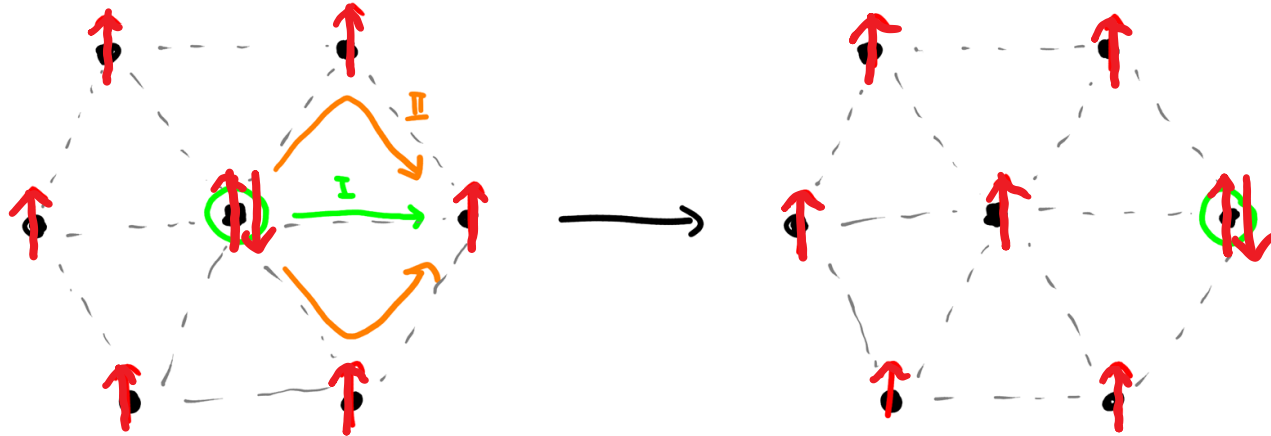


Electron moire magnetism for $\nu \sim 1$: determined by interactions or kinetic energy?

- For $\nu=1$, $\theta_{\text{CW}} \sim J = t^2/U \sim 0$, since $U=50$ meV and $t=1$ meV

Electron moire magnetism for $\nu \sim 1$: determined by interactions or kinetic energy?

- For $\nu=1$, $\theta_{\text{CW}} \sim J = t^2/U \sim 0$, since $U = 50 \text{ meV}$ and $t = 1 \text{ meV}$
- For $\nu > 1$, $\theta_{\text{CW}} > 0$: Nagaoka ferromagnetism (FM) with $\theta_{\text{CW}} \sim t$



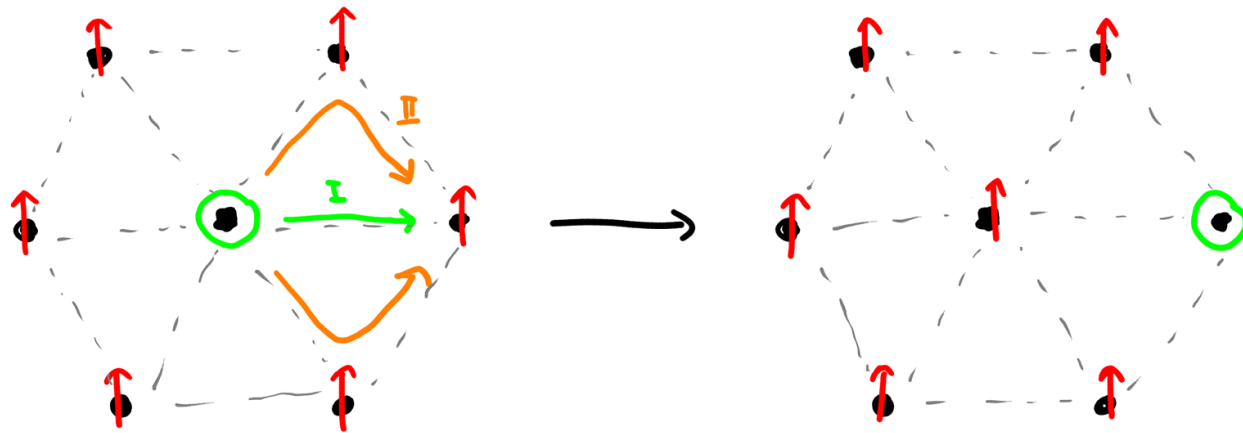
- Constructive interference of different paths if all spins are aligned

Electron moire magnetism for $\nu \sim 1$: determined by interactions or kinetic energy?

- **For $\nu=1$** , $\theta_{CW} \sim J = t^2/U \sim 0$, since $U= 50$ meV and $t=1$ meV
- **For $\nu>1$** , $\theta_{CW} > 0$: Nagaoka ferromagnetism (FM) with $\theta_{CW} \sim t$
- **For $\nu<1$** , $\theta_{CW} < 0$: kinetic Antiferromagnetism (AF) with $\theta_{CW} \sim t$, due to kinetic frustration in a triangular lattice

Antiferromagnetic correlations due to kinetic frustration

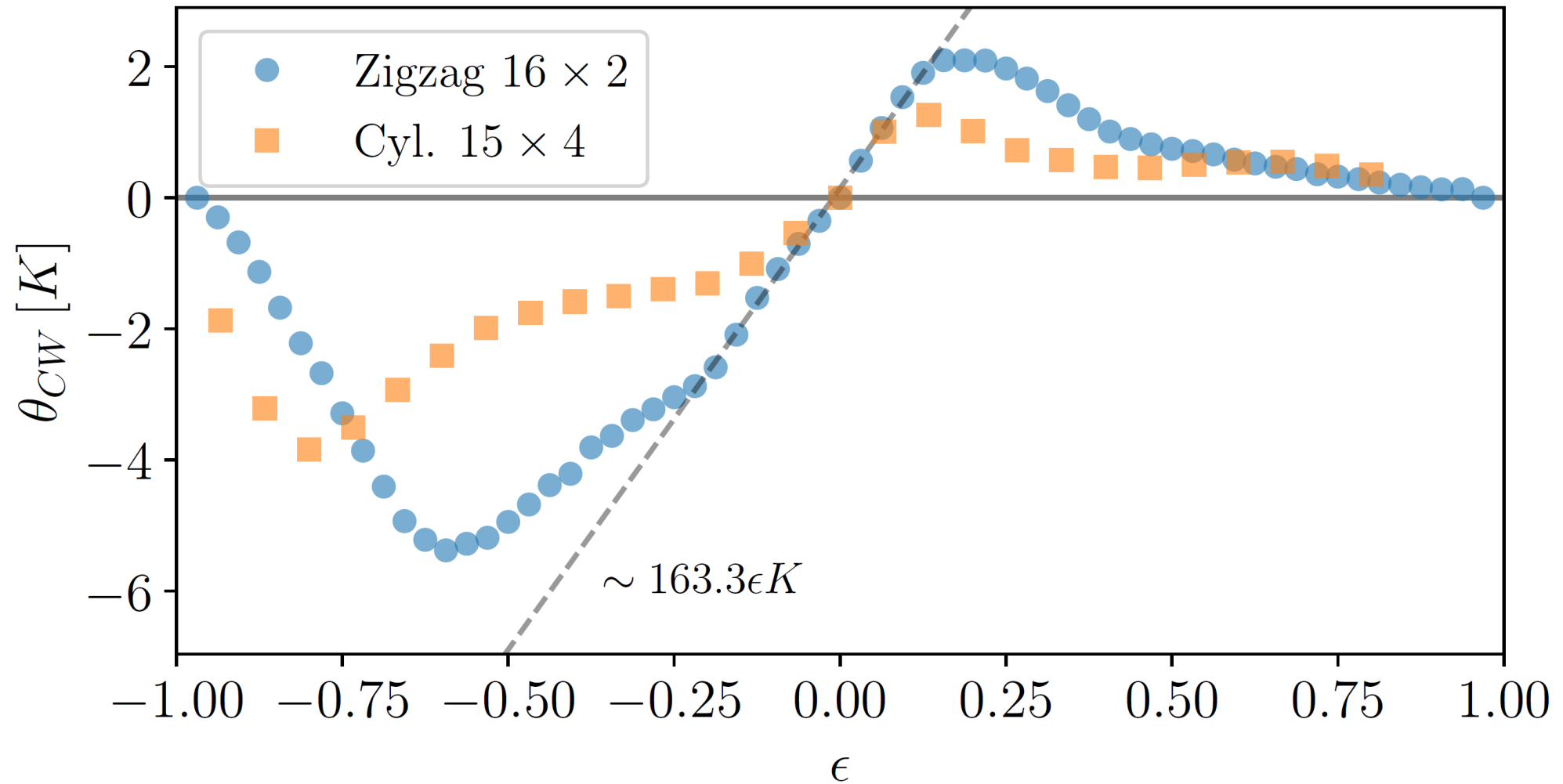
Fermi-Hubbard model for $\nu < 1$



→ Indistinguishable paths interfere destructively due to negative hopping t

→ Spin-polaron formation (hole bound to a spin-flip) allows for KE gain (Haerter&Shastry,Fu,Demler)

DMRG results (Morera & Demler)

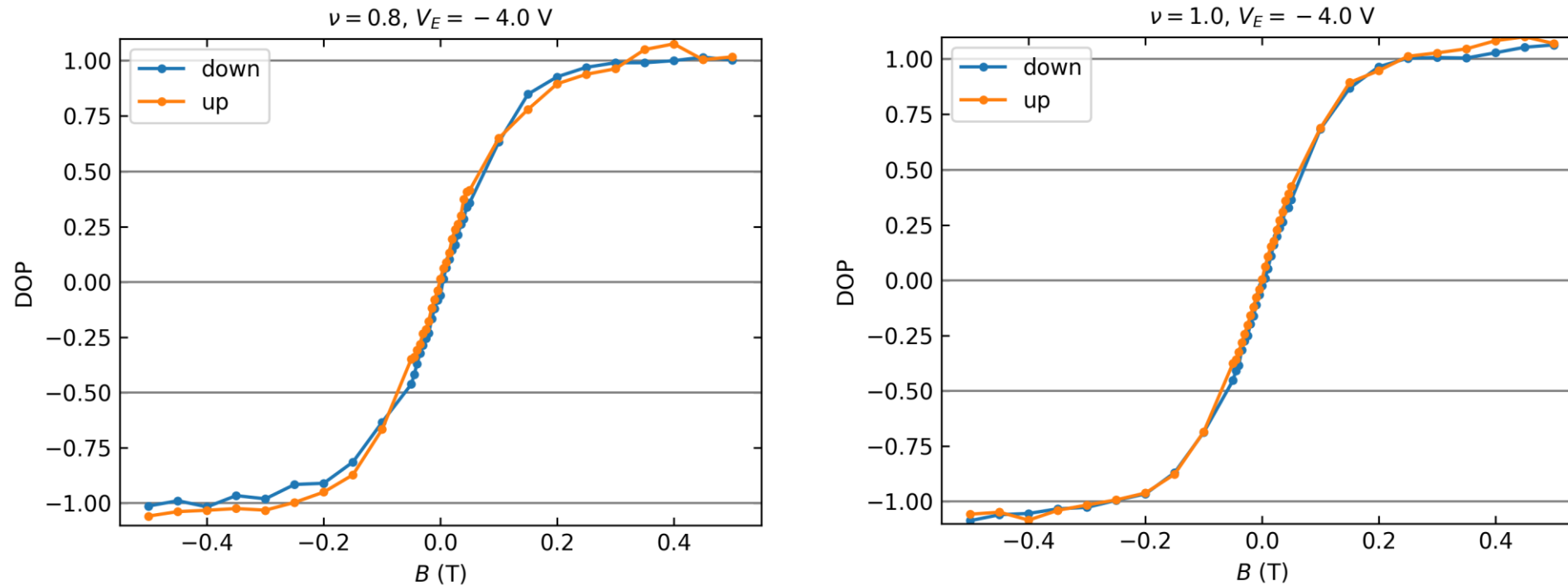


When Coulomb is replaced by infinite strength on-site repulsion (contact interaction), DMRG predicts a switch from AF to F limits

Experimental magnetization at $T < 500$ mK

Paramagnetic response for $\nu \leq 1$

~ 1 photon every 100 ns

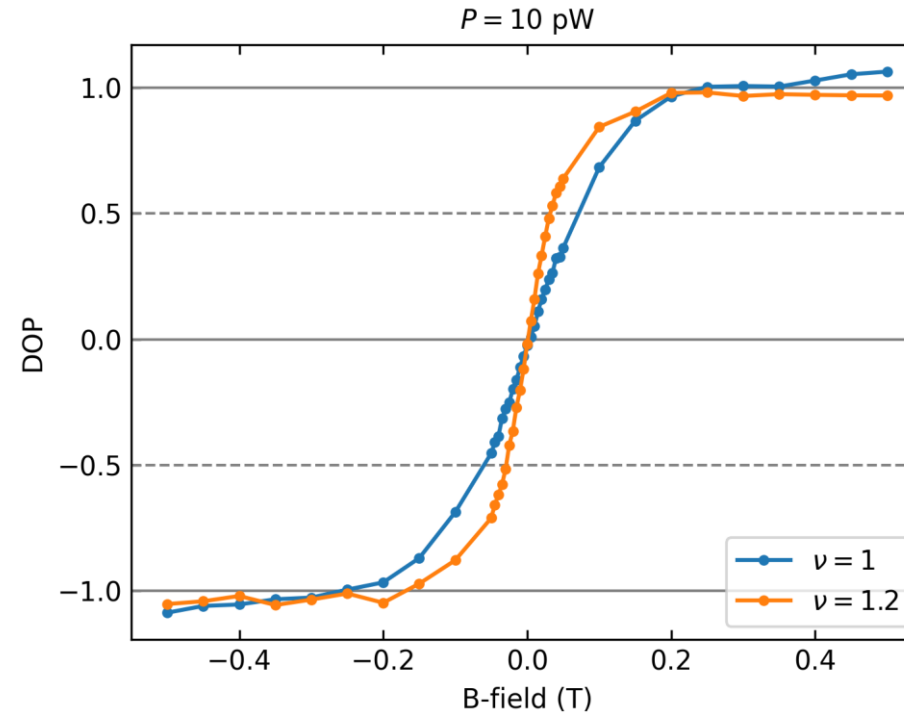
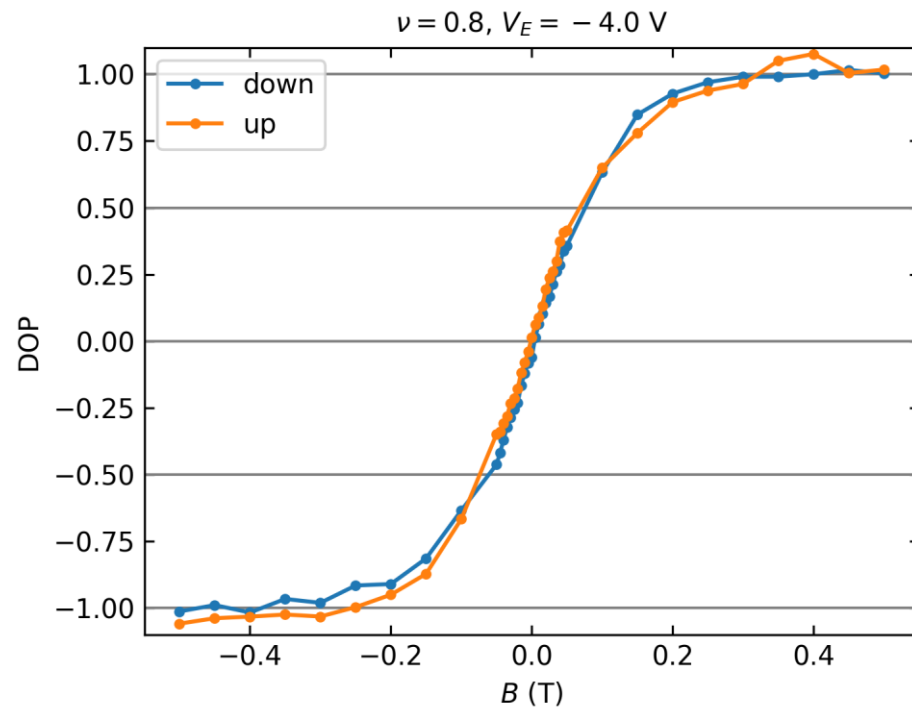


→ Degree of polarization (DOP) as a function of B identical for $\nu = 0.8$ and $\nu = 1$

Experimental magnetization at $T < 500$ mK

Enhanced susceptibility for $\nu > 1$

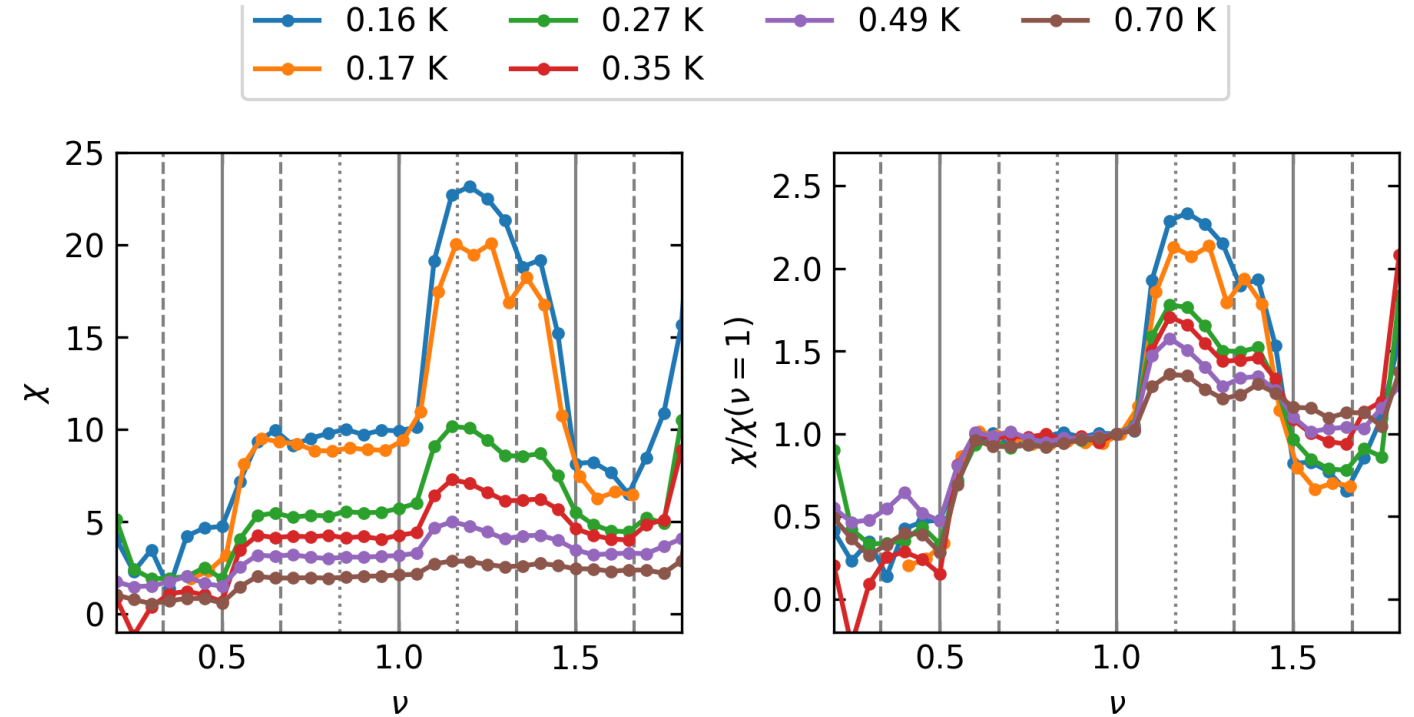
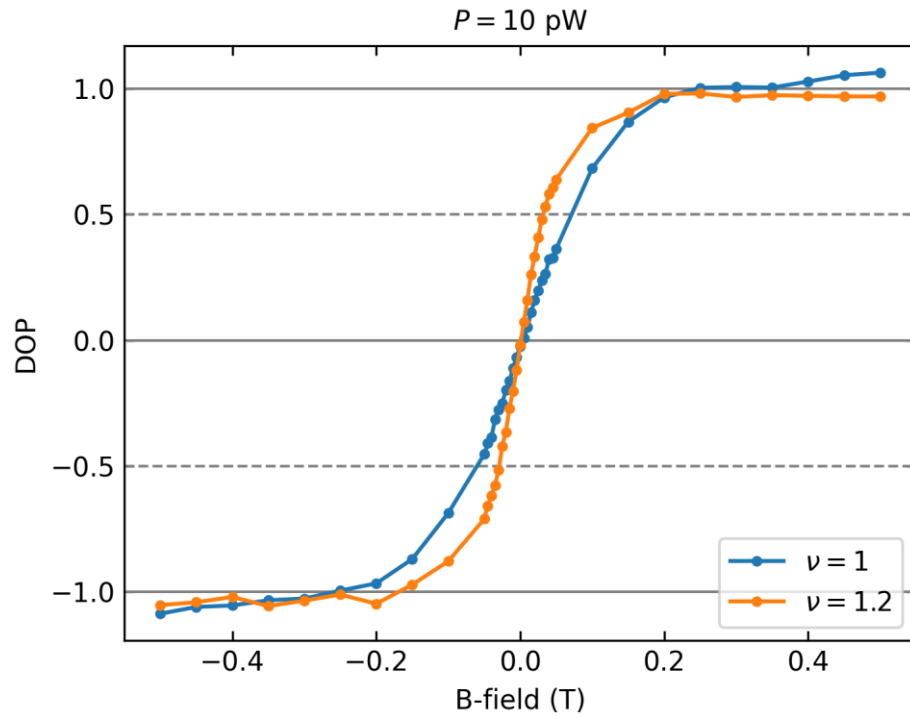
~ 1 photon every 100 ns



→ Degree of polarization (DOP) as a function of B identical for $\nu = 0.8$ and $\nu = 1$ but not for $\nu = 1.2$

Experimental magnetization at $T < 500$ mK

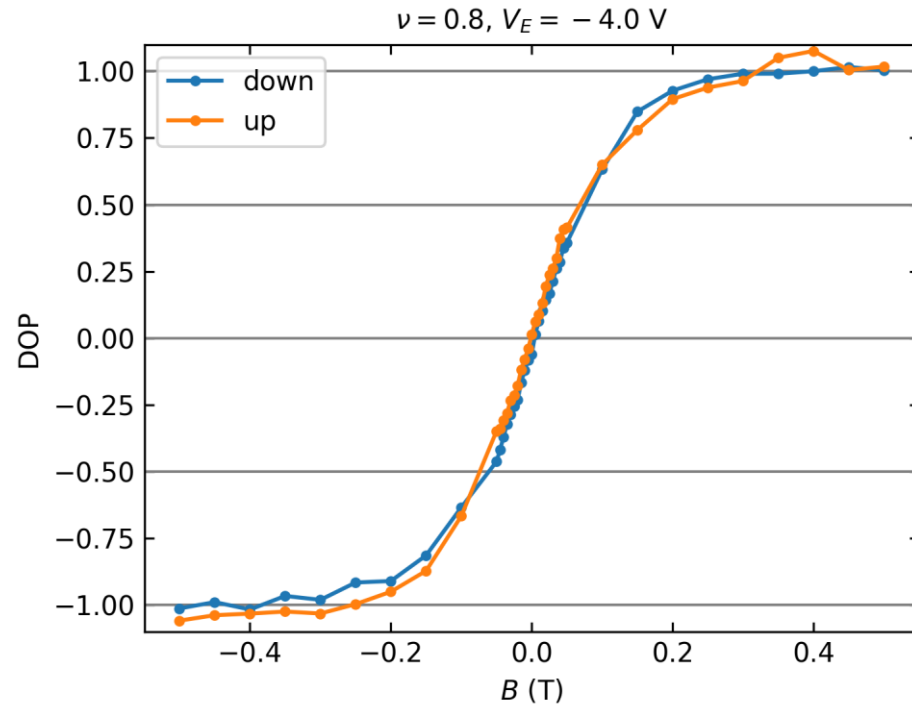
Enhanced susceptibility for $\nu > 1$ – Nagaoka mechanism



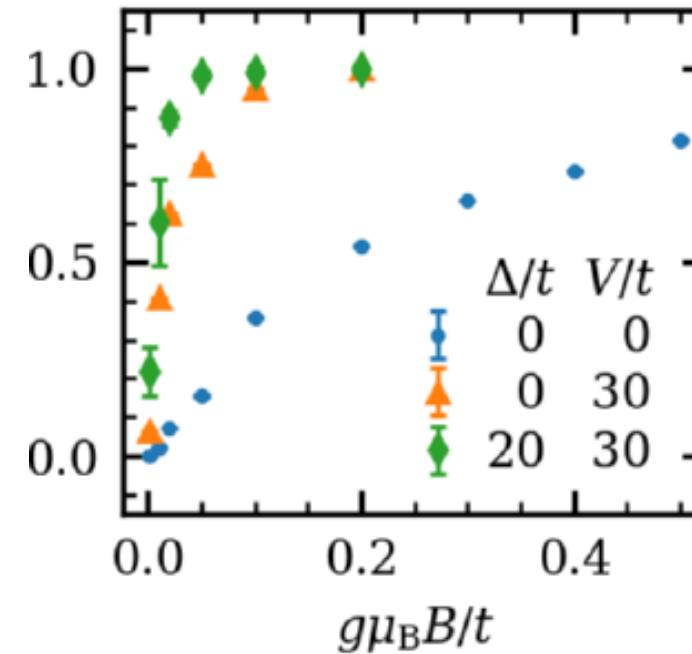
Sharp increase in spin susceptibility χ for $\nu > 1$

Experimental magnetization at $T < 500$ mK

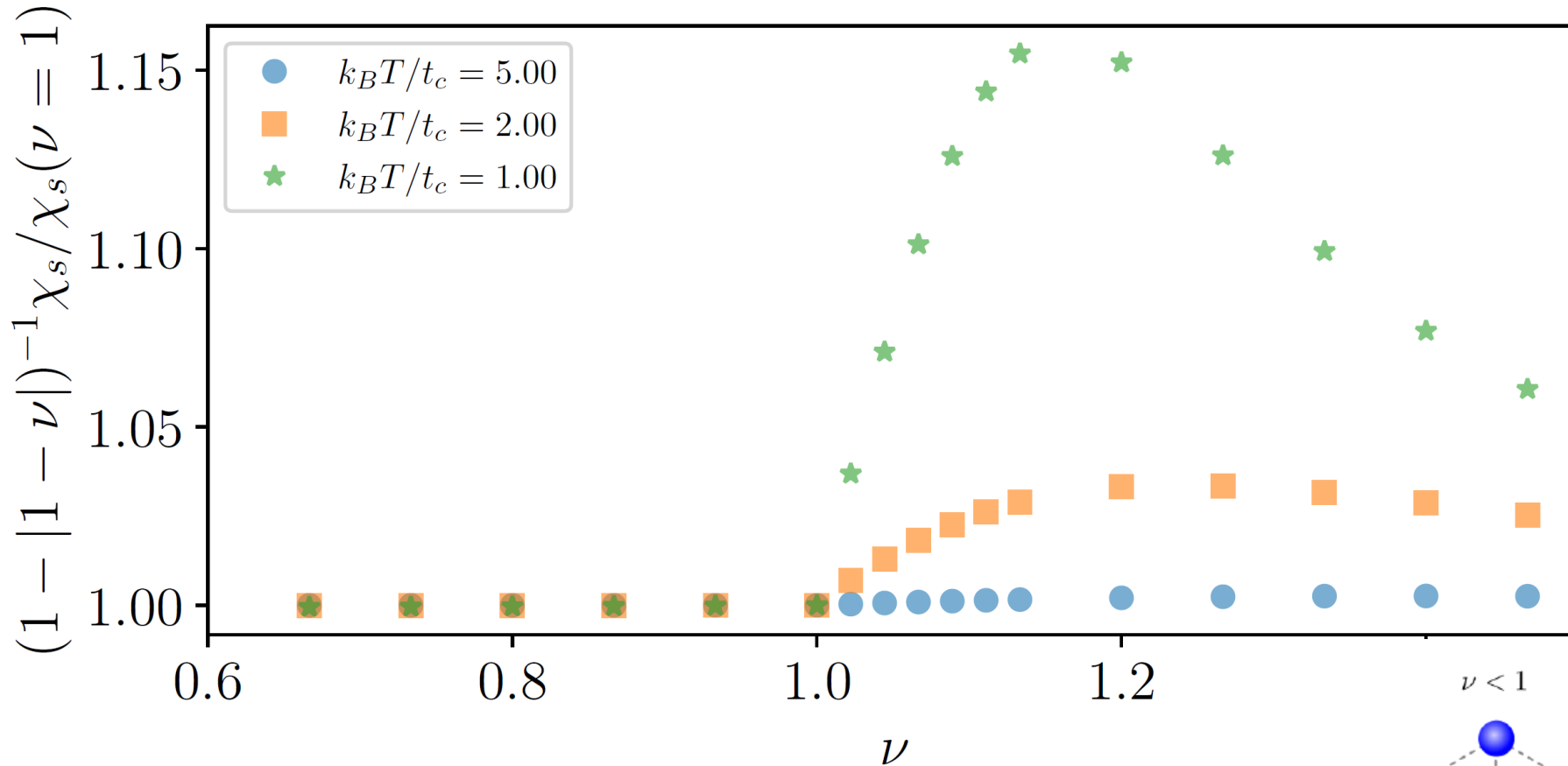
Paramagnetic response for $\nu \leq 1$ – Are long-range interactions the culprit?



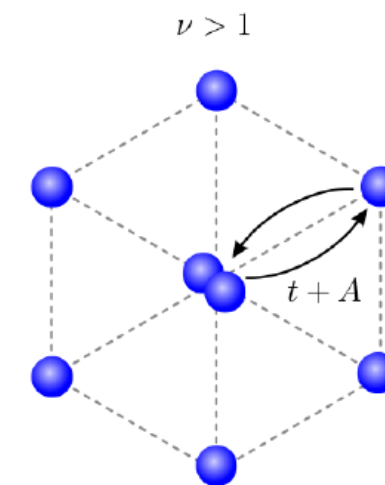
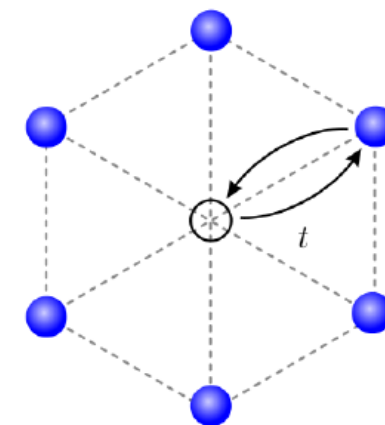
DMRG calculation of magnetization with NN interactions (V) and disorder (Δ)



DMRG with Coulomb assisted hopping

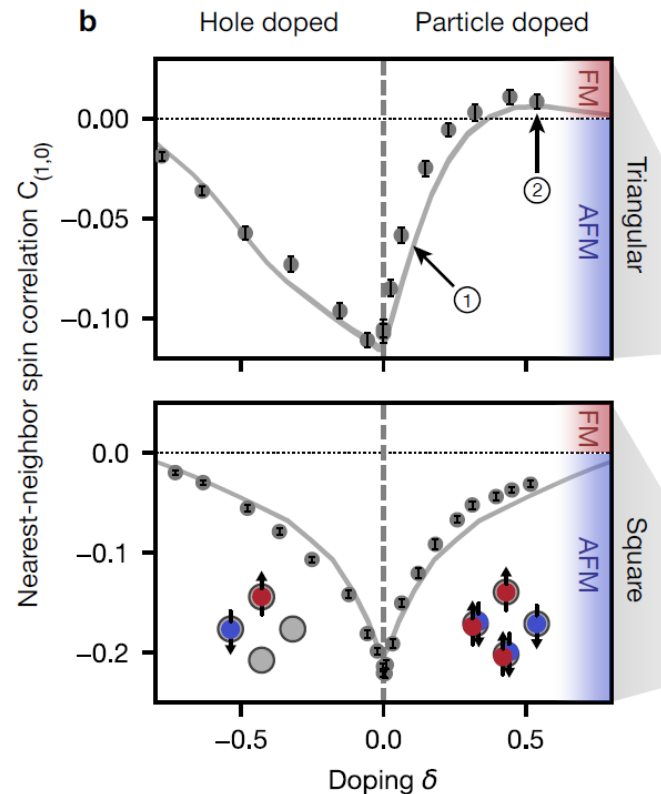


Long-range Coulomb interactions suppress AF correlations while enhancing FM through Coulomb assisted hopping



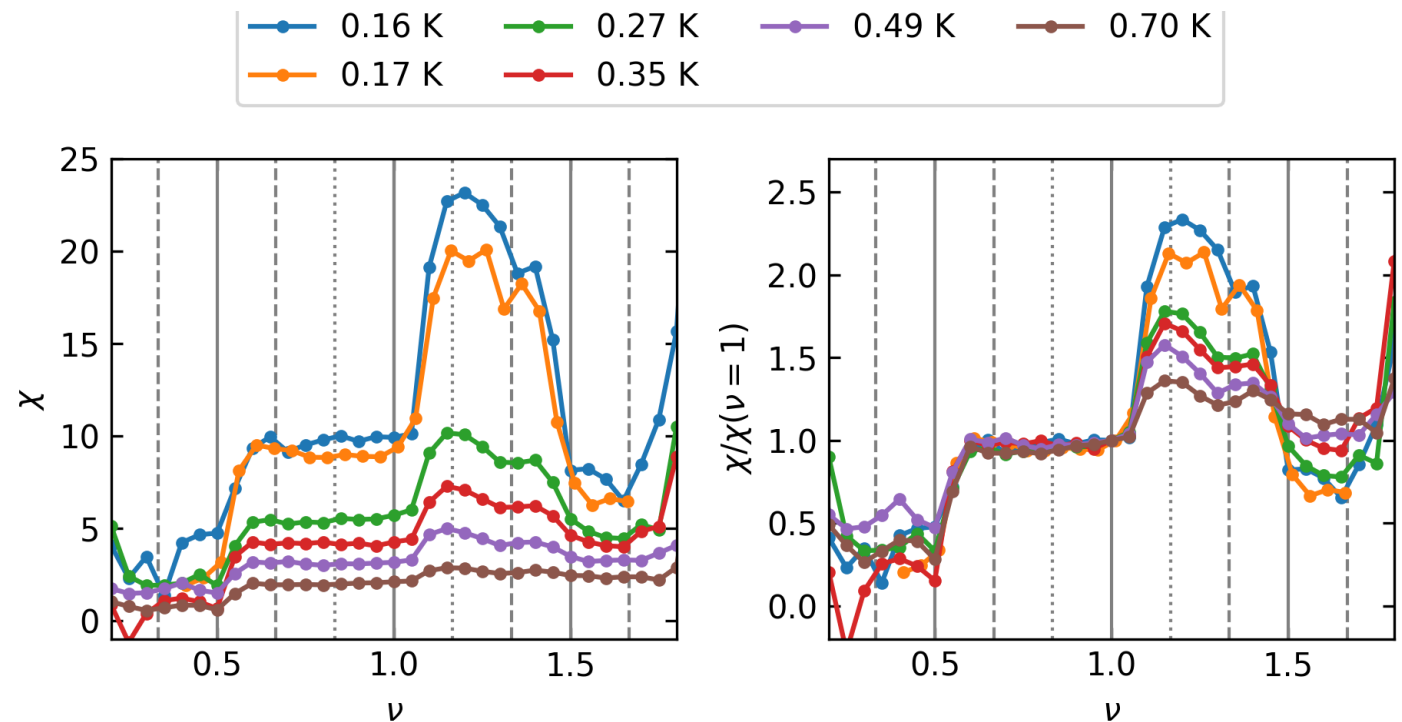
Quantum simulators of the Fermi-Hubbard model

- Kinetic magnetism in a triangular & square optical lattice of ultracold fermions (Greiner group)



- Strong AF correlations at $v=1$
- FM (AF) correlations for $v > 1$ ($v < 1$)
- Fully consistent with theoretical predictions

- Kinetic magnetism in triangular MoSe₂/WS₂ moire heterostructure



- Paramagnetic spin susceptibility for $\nu \leq 1$
- Nagaoka FM only for $\nu > 1$
- Long range Coulomb + disorder suppresses AF for $\nu < 1$

Summary and outlook

- Evidence for magnetism that originates from itinerant electrons minimizing kinetic energy – in stark contrast to usual magnetism which stem from electron-electron interactions.
- Future directions:
 - Chiral spin liquids using layer pseudo-spin
 - Kondo lattice